Superconducting Photon Detectors

Dmitry V. Morozov*, Alessandro Casaburi and Robert H. Hadfield

James Watt School of Engineering, University of Glasgow, Glasgow, Scotland

*James Watt School of Engineering, University of Glasgow, Glasgow, G12 8QQ, United Kingdom
Dmitry.Morozov@glasgow.ac.uk

Superconducting Photon Detectors

The ability to detect individual light quanta - single photons - is prized across many fields of physics from astronomy to quantum optics. Superconducting photon detectors offer exceptional performance in terms of sensitivity, spectral range and timing resolution. In this review we introduce the underlying physics of photon absorption in superconducting devices. We then present detailed case studies of contemporary superconducting detector technologies for photon counting at visible and infrared wavelengths. We conclude with a perspective on future developments in this exciting area.

1. Introduction

The purpose of this review is to introduce the physics and technology of superconducting photon detectors. Superconducting photon detectors can cover an exceptionally broad range of energies, from gamma rays (100 eV) through to terahertz (10^{-3} eV). Our primary focus is on single photon detection in the infrared range (energy around 1 eV or 1.6×10^{-19} J). This review is aimed at researchers entering the field, either interested in advancing the device technology or as end users seeking to select a suitable detector for a particular application. Our goal is to create a 'Field Guide' to superconducting photon detectors capable of operating in the single photon limit in the infrared wavelength range. We are indebted to previous reviews and edited compilations [1 - 16] and we hope that our work provides a useful and up to date perspective.

Section 2 covers essential background topics. In Section 2.1 we discuss the origin of the term 'photon' and how 21st century photon counting applications have become a significant driver for detector development. In Section 2.2 we introduce the phenomena of superconductivity and key theories. In Section 2.3 we expand the discussion to non-equilibrium superconductivity which describes photon absorption in superconducting materials. We link this theoretical discussion to the main detector types considered in Section 3. In Section 2.4 we discuss the range of superconducting materials, from elemental superconductors through to high temperature cuprate superconductors and emerging two dimensional superconducting materials. In Section 2.5 we discuss cooling requirements for superconducting detectors and current solutions.

Section 3 covers case studies of key superconducting photon detector types. In Section 3.1 we discuss the superconducting tunnel junction (STJ) detector. This consists of two superconducting electrodes separated by a thin tunnel barrier. A magnetic field is applied to suppress Josephson tunnelling, and photon absorption is monitored through the tunnelling of quasiparticles. In Section 3.2 we introduce the superconducting Transition Edge Sensor (TES). This consists of a superconducting device held at the temperature close to the abrupt superconducting transition from zero to finite resistance. When a photon is absorbed, a finite resistance is generated and a current is drawn and detected via a superconducting quantum interference device (SQUID) readout. Section 3.3 is focused on the Superconducting Nanowire Single Photon Detector (SNSPD or SSPD) which consists of a narrow superconducting wire which is cooled below the transition temperature and biased below the superconducting critical current. The SNSPD acts as an ultrafast switch, generating a voltage pulse when a photon is absorbed and recovering superconducting state very quickly. Section 3.4 covers the Microwave Kinetic Inductance Detector (KID or MKID). This device operates via the change in inductance of a superconducting strip when a photon is absorbed. The KID is embedded in a microwave readout circuit and the shift in resonant frequency is monitored. Section 3.5 introduces the superconducting Hot Electron Bolometer (HEB) which is an important device structure for low noise mixing at GHz frequencies and can in principle be adapted for photon counting at infrared wavelengths.

The review concludes with an Outlook Section 4. We discuss emerging trends and likely avenues for development and new applications in the coming decades.

When describing the operation principle of a single photon detector, it is very important to determine metrics to quantify how well it performs in generating an electrical signal upon absorption of a photon. Detectors cannot be sensitive to all photon energies. In the case of superconducting detectors it is not possible to detect photons with energy smaller than the binding energy 2Δ of the supercurrent-carrying Cooper pairs (where is the superconducting energy gap parameter $\Delta \sim \mathrm{meV}$ - see Section 2.2). In practice it is hard to detect individual photons with wavelength greater than $\lambda \sim 10$ μm. This is because not all the energy of a photon will be efficiently used for breaking of Cooper pairs and then for signal generation. Therefore, the upper cut-off wavelength of detection is usually reduced below this theoretical limit. Also, if the energy of the photon is too high it can pass through the detector without interacting with it or indeed can destroy it in the worst-case scenario. For these reasons, the **wavelength range** of operation is one of the first performance metrics to define when describing a photon detector. Another very important performance metric is the **detection efficiency** (η) that represents the probability that an output signal is generated upon the arrival of a photon at the detector. An ideal detector will have η = 100% in the wavelength range of operation but in practice η is always lower than 100% and is strongly dependent on the wavelength λ of the incident photons and on several other factors. In fact, photons can be lost before reaching the detector due to absorption, scattering or reflection within the experimental environment. These kinds of losses can be accounted for in the so-called coupling efficiency η_{coupling}. The ability of photon to be absorbed will depend on the material and design of detectors and this can be taken in account by defining the absorption efficiency $\eta_{\text{absorption}}$. Finally, once the photon has been successfully absorbed in the detector it may still be the case that occasionally no electrical output occurs. This non-unity probability might be affected by several factors that are all taken in account by defining the registering probability $\eta_{\text{registering}}$. Taking all these contributions into consideration, it is possible to define the overall **system detection efficiency:**

$$\eta_{\text{sde}} = \eta_{\text{coupling}} \times \eta_{\text{absorption}} \times \eta_{\text{registering}}$$

and this is commonly expressed as a percentage. For most photon counting detectors there is a finite probability of triggering an output pulse when no incident photon has been absorbed. This is known as the **dark count rate** (DCR) and is given the units of s^{-1} or Hz. The origin of dark counts depends on the detector type and operation mode. In superconducting detectors intrinsic dark counts triggered by electrical or thermal fluctuations can be very low. Stray light or blackbody radiation (due to the optical coupling scheme) may lead to an effective DCR due to background. If background events are low, the DCR may be bounded by rare events such as radioactive particles or muon absorption. The extent to which a photon detector can discriminate photons of different energies is called **energy resolution**. This performance metric is benchmarked as $\Delta E/E_0$, where ΔE represents the statistical error, the width of the statistical curve for repeated measurements, obtained by measuring photon at fixed energy E_0. This metric will also give information about what is the minimum difference in energy between two photons that can be resolved by the detector. The output signal level is well defined above the noise and the **signal-to-noise ratio** (SNR) is a measure that compares the level of an output signal to the level of background noise and is expressed as the ratio of signal power to the noise power. Higher SNR means that a signal can be discriminated much better above the background noise. The **noise-equivalent power** (NEP) describes the sensitivity of a single photon sensor and is defined as the signal power that returns a SNR equal to one in 1 Hz output bandwidth ($\mathrm{W}/\sqrt{\mathrm{Hz}}$). A smaller NEP corresponds to a more sensitive detector that can discriminate small amount of power from the noise or reduced average time. When the NEP refers to the output signal power generated in the detector, it is known as the electrical NEP; it is called the optical NEP when it refers to the optical signal power impinging on the detector:

$$NEP = \frac{h\nu}{\eta}\sqrt{DCR},$$

where h is Planck's constant and ν is the frequency of the photon. Timing properties for a single photon detector are also of great importance. For example, a detector will have a finite **recovery time** (τ) after detecting a photon, during which it is blind and not yet ready to detect a subsequent photon. This time interval sets a limit on the theoretical maximum count rate at which the single photon detector can operate and the performance metric to quantify this is defined as the response time. The overall recovery time in practice might be limited by other factors, such as the uncertainty in the photon arrival or the readout electronics. The recovery time is typically defined as the full width at half maximum (FWHM) of the detector output pulse or, in the case of a strongly asymmetric output pulse, the 1/e time constant of the recovery. Also with modern optical sources, the arrival time of a photon can be expected with high precision (much better than 1 ps). Typical single photon detectors have measurable uncertainty in the timing of the output electrical pulse which is used to register the arrival of the photon. In the context of photon counting this timing uncertainty is known as **timing jitter** and is the FWHM of the histogram produced over multiple photon arrivals with respect to an optical clock. There is also an observable time delay in the production of the output electrical signal from the detector, due to underlying physical processes or circuit dynamics, and this delay is known as **latency**.

2. Background

2.1 What is a photon?

The term "photon" was coined by G. N. Lewis in 1926 [17] and is defined as an elementary excitation of a single mode of the quantised electromagnetic field [18] The concept of quantised electromagnetic radiation [19, 20] was first introduced by Planck in 1900 to explain the black-body radiation spectrum [21], then used by Einstein in 1905 to explain the photoelectric effect [22 - 24] and also by Compton in 1923 to explain the wavelength shift of scattered X-rays [25]. The energy of a photon is given by:

$$E = h\nu = \frac{hc}{\lambda},$$

where h is Planck's constant, ν is the frequency, c is the speed of light in vacuum and λ is the wavelength.

Now, a century later the possibility to detect these single quantum objects is vital for a host of applications at the frontiers of science and technology. Photon counting can be achieved at visible and infrared wavelengths with devices such as photomultipliers (PMTs) and semiconductor single photon avalanche diodes (SPADs) [3]. The requirement to detect and count single photons with very high efficiency, speed of operation, high timing resolution and low noise, as photon energies drop at infrared wavelengths, brings superconducting photon detectors into consideration. We can divide photon counting applications into two broad groups. Firstly, applications where individual photons are used as quantum bits or 'qubits' to encode, manipulate, transfer and measure information to enable computation and potentially unconditionally secure communication [26]. These represent a major driver of the current research into single-photon detectors, demonstrated by the explosive growth of the field of optical quantum technologies over the last few decades [27, 4]. Secondly, there are numerous applications where single photon sensitivity is required to work in "photon starved" environments or with a faint light source. In the life sciences domain, these can include applications such as fluorescence lifetime measurements (FLIM), single molecule spectroscopy, bioluminescence detection [28], DNA sequencing [29], Förster resonance energy transfer (FRET) for studying protein folding [30], diffuse optical tomography [31, 32] and singlet oxygen dose monitoring [32] for photodynamic therapy for the treatment of cancer. A major emerging area is single photon remote sensing, in particular light detection and ranging (LIDAR) for depth imaging and spectroscopy [33] and fibre optic remote sensing techniques optical time domain reflectometry [34], and fibre Raman temperature sensing. Deep space optical communications require photon counting receivers [35]. Infrared photon counting is a key component of picosecond imaging circuit analysis, systems for the semiconductor industry [36]. Photon counting has a long history in observational astronomy from UV to far infrared [1] and new applications are emerging such as exoplanet spectroscopy and dark matter searches [37]. Hence, infrared single photon detectors are crucial for a host of modern scientific applications. The past few decades have seen the advancement of ever more sophisticated technologies to satisfy the performance demands of these emerging applications. As we show in this review superconducting photon detectors in different forms can be tailored to the requirements for the most challenging photon detection applications.

2.2 *Superconductivity*

The combination of unique characteristics in superconducting materials, and the extremely low thermal noise conditions available in cryogenic environments, has long made superconducting devices attractive for ultra-low noise detection. Superconducting photon detectors can offer unrivalled performance in terms of high sensitivity, high efficiency, timing properties, spectral resolution and excellent signal-to-noise ratio.

Superconductivity was discovered in 1911 when Heike Kamerlingh Onnes found that the resistance in a solid mercury wire cooled down below a critical temperature T_c = 4.15 K suddenly vanished [38]. It was only in the 1950's that comprehensive theoretical models were developed to take into account the experimental observation of perfect diamagnetism (known as the Meissner effect) [39] and explain the quantum nature of several phenomena like fluxoid quantisation [40] . The thermodynamic model developed by Ginzburg and Landau (GL) [41] describes superconducting state in terms of an Order Parameter representing a condensate of superconducting charge carriers, having mass m^* and charge e^*, that satisfy the minimisation of Gibbs free energy equations around the critical temperature, $T \sim T_c$. This provides a derivation for the London equations [42] (a phenomenological model developed in 1935 that considers the magnetic behaviour of superconductors). In the GL model it is possible to find the magnetic penetration depth λ_L, defined in the London theory as characteristic length over which the magnetic field (superconducting shielding current) penetrates and decays to zero in a bulk superconductor. It is also possible to naturally define the other fundamental length, the coherence length ξ_{GL}, over which the superconducting charge carrier condensate can vary appreciably. In 1962 Brian Josephson predicted tunnelling between two regions of superconductor separated by a thin barrier, the 'Josephson effect', that was experimentally verified soon after [43, 44]. The present microscopic understanding of "conventional" superconductivity is based on the BCS microscopic theory [45, 46] proposed by J. Bardeen, L. Cooper, and J. R. Schrieffer in 1957 (Nobel prize in 1972). In the BCS theory, developed in the second quantisation formalism, it is assumed that bound electron pairs with opposite antiparallel momentum and spin - Cooper pairs - are formed due to an effective attractive electron-electron potential. In conventional superconductors the potential is mediated through exchange of virtual phonons (deformation of reticular lattice in the material due to interaction with electrons) that gives rise to an attractive potential and forms an energy gap 2Δ in the density of states centred on the Fermi level E_F (see Figure 1). Δ is the superconducting gap parameter and can also be viewed as the energy required to excite each electron in the Cooper pair. The Cooper pairs thus formed are Bosons, they condense at the Fermi level E_F. The Cooper pair binding energy is 2Δ. The Cooper pairs behave coherently as single condensate that can be described by a single wavefunction or order parameter. This underlying microscopic process is responsible for the observed transport, magnetic and quantum behaviour of superconductivity as a new state of matter.

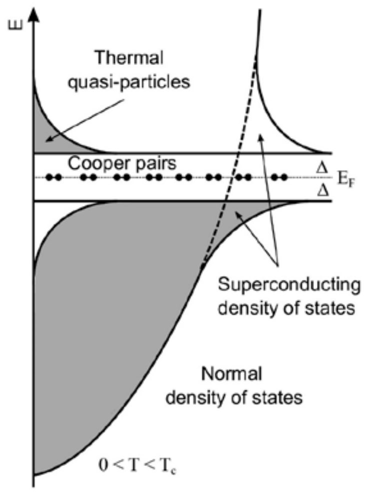

Figure 1. Dependence of the superconducting (solid line) and normal (dashed line) densities of states over a broad energy range. This energy diagram corresponds to temperature $0 < T < T_c$, the dashed area represents the occupied states. Δ is the superconducting energy gap parameter and E_F is the Fermi energy. The binding energy of a Cooper pair is 2Δ. In the finite temperature range, Cooper pair breaking is continuously happening due to thermal excitation; at equilibrium this is balanced by Cooper pair recombination. Δ is both temperature and magnetic field dependent. In the BCS theory $2\Delta\,(T=0) = 3.52\ k_B T_c$ and the value Δ of drops rapidly to zero as T approaches T_c.

At $0 < T < T_c$, due to thermal noise there are some electrons that are not paired occupying energy states above the gap. These unpaired electrons are termed "quasi-particles": elementary excitations above superconducting ground state defined as the superposition of negatively charged electrons and positively charged electron holes. Quasi-particles are Fermions. Gor'kov showed that the GL theory is a limiting case of the BCS theory and it can be formally derived from it for $T \sim T_c$ using $m^* = 2m$, $e^* = 2e$ and the coherence length at zero temperature $\xi_{\mathrm{BCS}} \approx \frac{\hbar v_{\mathrm{F}}}{\pi\Delta}$ to represent the mass, charge and average size of Cooper pairs within the superconductor [47]. Superconductors have a range of unique properties that can be exploited in technological applications. The superconducting state vanishes abruptly above the superconducting transition temperature T_c, giving a sharp resistance versus temperature transition curve between the superconducting and normal state. Superconductors show a state with zero DC resistance that can be destroyed if the flowing current is increased above a threshold or critical value, I_c. Superconductors show complete magnetic expulsion/repulsion under certain circumstances. Superconductors show an additional "kinetic inductance" $l_{\mathrm{k}} = \frac{m}{n_{\mathrm{s}}e^2} = \mu_0\lambda_{\mathrm{L}}^2$ that depends on the density of Cooper pairs in the material (current and temperature). The binding energy of the Cooper pairs is twice the value of the superconducting energy gap parameter Δ which is of order of ~meV in low temperature superconductors, about ~1000 smaller than the bandgap in typical semiconductor materials (~ eV). Also, superconductors show some peculiar macroscopic quantum phenomena like fluxoid quantisation where magnetic flux penetrates in a superconductor in quantised form $\phi_0 = 2.067 \times 10^{-15}$ Wb (as Abrikosov vortices [48]) called magnetic flux quanta. The Josephson effect, a quantum tunnelling effect, can be observed in barrier junctions [49] or weak links [50] where Cooper pairs tunnel with zero dissipation showing a distinctive non-linear current-voltage characteristic.

2.3 Non-equilibrium superconductivity and photon detection

These unusual properties can be harnessed in superconducting photon detectors. These devices can be placed in several classes depending on the detection scheme employed. They all hinge on the fact that interacting photons break Cooper pairs and only differ in how the induced non-equilibrium is used for measurement. Different measurements schemes are chosen to optimise different performance characteristics required in particular applications. It is therefore important to understand what happens when a photon interacts with a superconductor and how the photon energy $h\nu$ compares with the superconducting energy gap parameter Δ. In principle, a photon can be detected if its energy is larger than the binding energy of Cooper pairs $h\nu > 2\Delta$ (Figure 1).

A superconducting material at thermal equilibrium can be described by three coexisting sub-systems: Cooper pairs, quasiparticles and phonons (of the superconductor and substrate). All three systems are in thermal equilibrium and their equilibrium distribution functions are at the same temperature [51]. An external perturbation such as a photon with energy $E_0 = h\nu$ can drive one of the sub-systems out of equilibrium depending on the value of E_0 [52]. The energy down-conversion following the interaction with an energetic photon is generally accepted to occur in four distinct stages (see Figure 2) [53]. In the first stage (I), the energy absorbed in the superconductor destroys the equilibrium of one sub-system generating energetic photoelectrons [54]. These electrons generate a certain number of secondary high-energy electrons (hot electrons) and in this stage strong electron-electron scattering with a characteristic interaction time $\tau_{\text{e-e}}$ dominates the energy down conversion mechanism. After a few $\tau_{\text{e-e}}$ the hot electrons thermalise to an energy $E_1 \simeq \hbar\omega_D$ (where ω_D is the Debye frequency) defining the end of the first stage.

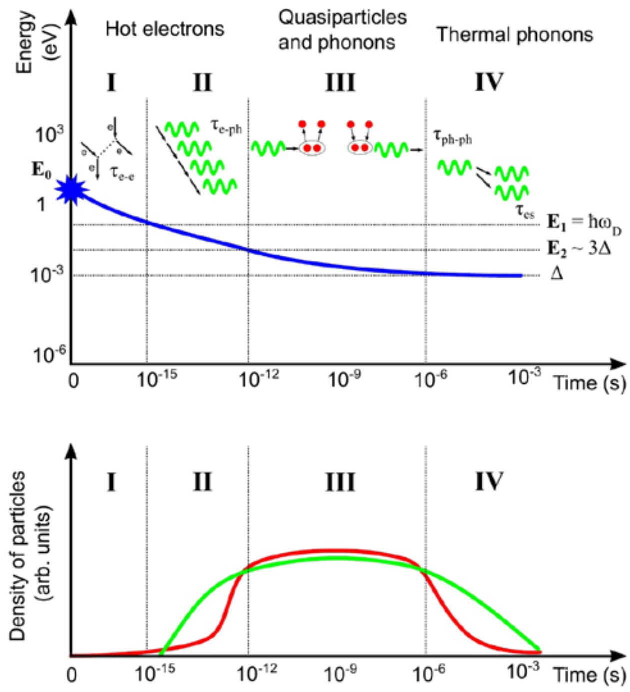

Figure 2. Thermalisation scheme showing subsequent channels of the energy transfer and behaviour of the subsystem populations in a superconductor that relaxes towards equilibrium, following the interaction with an energetic photon having energy E_0. The cascade of processes is described in four stages (I - IV). The hot electrons created upon photon absorption dominate stages I and II, transferring energy to quasiparticles and phonons in stage III. Energy dissipation as thermal phonons is completed in stage IV. In this qualitative illustration, the photon energy E_0 is ~1eV, an order of magnitude above the Debye energy $\hbar\omega_D$, which is in turn much greater than the superconducting energy gap parameter Δ ~10^{-3} eV. In the upper plot, the energy per particle (for hot electrons moving to quasiparticles) is shown against time. In the lower plot the particle densities (quasiparticles - red, phonons - green) are illustrated versus time.

The second stage (II) of energy down-conversion takes the non-equilibrium electron distribution down to a second characteristic energy $E_2 \sim 3\Delta$ where electron-phonon scattering with a characteristic time $\tau_{e\text{-}ph}$ becomes stronger than the electron-electron scattering ($\tau_{e\text{-}ph} < \tau_{e\text{-}e}$) and the energy down conversion process releases many energetic phonons clustered at the Debye frequency, ω_D. At this point (as illustrated in the lower plot of Figure 2) the quasiparticle population (red curve) responds very quickly compared to the slowly varying phonon distribution (green curve) because of the much higher electronic scattering rate. The final distribution at the end of stage II is a non-equilibrium population of high energy phonons and quasiparticles. Over the third stage (III) the mixed distribution of quasiparticles and phonons evolves to a quasiparticle distribution centred at the superconducting gap edge through: i) the Cooper pair breaking process (with phonon absorption), ii) recombination of two quasiparticles in a Cooper pair (with phonon emission) and iii) phonon escape in the substrate. Stage III ends when the energies of the emitted phonons fall below 2Δ and the energy per quasiparticle approaches Δ. These phonons are unable to break Cooper pairs halting the creation of quasiparticles. Finally, in the fourth stage (IV) only phonons with energy smaller than 2Δ are present and the system returns to the initial state of equilibrium (bath temperature) through the processes of phonon-phonon scattering and phonon escape through the substrate with τ_{es}. Depending on the measurement scheme, the properties of the superconducting material used and device design; it is possible to generate different output signals for detection. Even though various detection schemes rely on capturing non-equilibrium particle temperatures at different stages in the energy down-conversion process (Figure 2) all these detection methods fundamentally rely on the Cooper pair breaking mechanism. In principle, superconducting photon detectors - SPDs - can be classified in two main categories: Bolometers and quantum or particle detectors. For this topical review we highlight the most widely used SPDs at the time of writing: superconducting tunnel junction (STJ), transition edge sensor (TES), superconducting nanowire single-photon detector (SNSPD), kinetic inductance detector (KID) and hot electron bolometer (HEB). The detection mechanisms are discussed and contrasted in this section. Detailed case studies with in-depth discussion the state-of-the-art and applications are included in Section 3.

The STJ is based on a Josephson junction device structure consisting of a thin insulator sandwiched by two superconducting layers acting as electrodes. In operation as a photon detector, one of the superconducting electrodes of the STJ absorbs the photons and the energy is converted into quasiparticles (arising from broken Cooper pairs) and phonons [55]. This STJ also operates in the sub-Kelvin temperature range and relies on the detection of tunnelling of quasiparticles generated in the third stage of energy down-conversion from the absorbing electrode to the other electrode. That is why the STJ time constant lies in the range of few μs or less (depending on the electrode area). A magnetic field is required in its operation to suppress the Josephson tunnelling of Cooper pairs [56].

The superconducting TES concept arose from earlier work on low temperature silicon microbolometers for X-ray spectroscopy [57]. The TES is usually created from a low-temperature superconducting film acting as absorber and/or thermometer embedded in an electric circuit which produces a very sensitive resistive change within its sharp normal-to-superconducting transition upon photon absorption. This scheme also operates in the sub-Kelvin temperature range relying on the detection of equilibrium phonons generated in the fourth stage of energy down-conversion and is relatively slow but can give very high photon detection efficiency and photon energy or photon number resolution [58]. The use of voltage-bias and superconducting quantum interference device (SQUID) readout both contribute to the response time of TES detectors and make them more stable and suitable for practical implementation in large arrays [59].

A KID consists of a superconducting microwave resonator, in a lumped-element or distributed design. The resonance frequency and internal quality factor (Q) change due to the variation of kinetic inductance resulting from the change in quasi-particle density due to Cooper pairs breaking following photon absorption. The frequency shift and internal dissipation signal measurements (in-phase and quadrature [I-Q] microwave signal measurement) allow readout of large numbers of KID devices on a single microwave feed line with frequency multiplexing [60, 61]. This scheme also operates in the sub-Kelvin temperature range and relies on measurements of quasi-particle generated (Cooper pair breaking) in the second and third stage of energy down-conversion. KID devices have the potential to reach very fast response speeds, but current KID multiplexing schemes do not allow operation at frequencies much greater than 1 kHz [62]. STJ and KID devices exhibit optical photon detection ability; however, no practical detectors have yet been developed in the infrared wavelength range.

A SNSPD is generally comprised by a very thin and small width strip that is cooled down well below its T_c and it is current biased at an operating value slightly smaller than its critical current: $I_b \lesssim I_c$. When a photon is absorbed by the strip, an ultra-fast voltage pulse is generated [63]. Depending on the choice of superconducting material, the energy gap, kinetic inductance and operating temperature of the SNSPD can be tuned. Typical SNSPD devices operate in the temperature range 0.8 - 4 K [64]. The SNSPD relies on the generation of quasiparticles in the first and second stage of energy down-conversion. These quasiparticles are confined in the small width of the strip, rapidly destroying superconductivity generating a short-lived resistive region (commonly known as a “hot-spot” or nucleating vortex-antivortex pairs) [65 - 67]. SNSPD devices are very fast, with a recovery time as low as a few nanoseconds and exceptionally low timing jitter (down to a few ps) [68, 69]. SNSPDs can be optimised for near unity photon detection efficiency (comparable to the TES) [70].

The HEB bolometer utilises the generation of “hot-electrons”, the high energy quasiparticle distribution in region I of Figure 2, due to photon absorption in thin superconducting films with metallic behaviour in their normal state (Nb, NbN, Al, Ti etc) [71, 72]. Thermalisation of these hot electrons or quasiparticles can occur either through generation of phonons or by diffusion through the metallic contacts depending on the choice of superconducting material, film thickness, design and electron-phonon coupling strength. This choice will determine the sensitivity and the response time of the photon detector. The typical operation temperature for HEB detectors is sub-Kelvin, usually about tens of mK, and it relies on the measurement of the resistance change caused by the excess of hot electrons.

2.4 Materials for superconducting photon detectors: a brief introduction

A detailed model describing the detection mechanism in SPDs is not only of fundamental interest but also allows us to understand how the material parameters influence the detector properties. This insight helps identify the best possible superconducting material for a specific application. In all the photon detection schemes under consideration in this review, the starting point is the absorption of the photon in the superconducting structure. This absorption is mainly governed by the optical properties of the superconducting material, and the surrounding dielectric and metallic layers. The superconducting energy gap parameter Δ and the Cooper pair binding energy 2Δ are important to consider when choosing materials of the detector because this will affect the sensitivity and efficiency: smaller Δ means that a larger number of Cooper pairs can be broken for a given photon energy. As we have seen, following from the BCS theory, materials with smaller Δ also have lower critical temperature T_c. However, other factors come into play depending on the detection scheme and the intended application.

With the exception of SNSPDs, SPDs usually operate at sub-Kelvin temperatures, not only for the chosen materials to be in superconducting state, but also in order to achieve a better signal-to-noise-ratio.

STJs must be operated at temperatures well below the superconductor's critical temperature (typically well below 1 K) to guarantee that the equilibrium state of the junction is easily perturbed by any photon striking it and an electrical charge proportional to the energy of photon can be easily extracted from the device [73]. For these detectors, the materials commonly used are niobium (Nb), tantalum (Ta), aluminium (Al) or hafnium (Hf). There is a distinction between the larger energy gap materials chosen for the absorber (Nb, Ta) that maximise photon absorption and the smaller energy gap materials (Al, Hf) used for fast tunnelling of quasi-particles created in the junction and to improve energy resolution thanks to their smaller energy gap.

For a bolometric detection of infrared photons the presence of fundamental thermal noise requires operation temperatures below 1 K. Most of the TES devices work in the 100 - 200 mK temperature range and common materials used are tungsten (W), titanium/gold bilayer (Ti/Au) or hafnium (Hf) because of the tunability of the T_c in the ~ 100 mK range and also for their relatively weak coupling between electron and phonon systems (small heat capacity) at these temperatures [74]. In this scheme, materials with higher T_c will have faster recovery time.

For the KIDs, it is important to design resonators with smaller surface resistance in order to obtain the highest Q-factor possible and to maximise the number of quasi-particles created upon photon absorption [75]. The surface resistance of the superconducting material depends on the energy gap but also on the residual resistivity (the resistance just above T_c) as well. That is why devices are typically operated at few hundreds of mK and materials are chosen to have low residual resistivity, longer quasi-particle lifetime in addition to a small energy gap, and the most commonly used materials for KIDs are aluminium (Al), niobium (Nb), titanium (Ti) or titanium nitride (TiN).

For SNSPDs, materials with a smaller energy gap will allow detection of photons with smaller energy and to saturate the detection efficiency at lower bias current, giving negligible dark counts [76]. Their kinetic inductance will affect the response time and their critical current density and normal state resistivity will affect the amplitude of the output signal. The most commonly used materials for SNSPDs [6] are niobium nitride (NbN), niobium titanium nitride (NbTiN) for operation at T = 2 - 4 K, and tungsten silicide (WSi) or molybdenum silicide (MoSi) for sub-Kelvin operation with higher efficiency but slower operation.

For HEB detectors, the most popular materials are aluminium (Al), titanium (Ti), niobium (Nb), niobium titanium nitride (NbTiN) etc., due to their metallic behaviour [77]. Materials with a short electron-phonon coupling time constant (such as NbTiN) are most promising for HEBs. A short mean free path and small coherence length allows thinner superconducting films to be employed increasing the HEB sensitivity.

The discovery of new superconducting materials is of definite interest for SPD development. Cuprate high T_c (high-T_c materials) have been explored extensively for bolometric detection applications but achieving single photon sensitivity in the infrared is challenging, due to the larger energy gap and materials processing issues [78]. Magnesium diboride (MgB_2) shows a critical temperature T_c ~ 40 K, with small residual resistivity of $\rho = 0.1$ µm×cm, small kinetic inductance per square L_k (4.8 K) = 1.3 - 1.6 pH/□ and two energy gaps $\Delta\sigma$ and $\Delta\pi$. This material has been successfully used to demonstrate operation of KIDs [79] and SNSPDs [80] at higher temperatures.

In addition to the operating requirements for different detection schemes, other factors play a role in the practical advancement of superconducting detectors. The versatility of the material to be grown as a thin film or patterned for specific detector fabrication, stability in different environmental conditions and during routine thermal cycling required for operation can play a major role in its choice for detector applications. This is why MgB_2 has not been widely adopted or why other high-T_c materials like Yttrium Barium Copper Oxide (YBCO, T_c = 91 K) have not yet realised the dream of operating these detectors at liquid nitrogen temperature (77 K) [81, 82].

In conclusion, the choice of superconducting material for SPD devices is not always straightforward but is more likely to be a trade-off between several considerations to optimise the performance of detectors for specific applications. Below in Table I we present the most common materials used for the SPDs described in this review with relative critical temperatures and the 2Δ ($T = 0$) values for bulk material.

Table 1. List of most common materials used for the fabrication of superconducting photon detectors (SPDs), with their bulk T_c and bulk value of 2Δ (at $T = 0$). As illustrated in Figure 1, Δ is the superconducting energy gap parameter and the Cooper pair binding energy is 2Δ.

Material	α-W/β-W [74]	Hf [83]	Ta [83]	β-Ta [83]	Ti/TiN [83]	Al [83]	WSi [84]	MoSi [84]	Nb [85]	NbN [85]	NbTiN [85]	MgB_2 [85]	YBCO [83]
T_c (K)	0.015/2	0.13	4.5	0.6	0.8/4.5	1.2	5	7.5	9.26	16	16	39	85
2Δ (meV)	0.0045/0.6	0.04	1.4	0.18	0.2/1.4	0.4	1.5	2.3	3.3	4.9	5.1	6.8, 1.8	30

2.5 Cooling for superconductors: the challenge of cryogenics

The excellent performance of SPDs makes them ideal candidates for a wide range of emerging applications but their widespread adoption has always been closely connected to the development of cryogenic technology [86]. Nowadays it is no longer necessary to use liquid cryogens such liquefied helium (He) which boils at $T = 4.2$ K under atmospheric pressure to cool and operate superconducting detectors. This is thanks to the development of practical closed-cycle cryocoolers that exploit the thermodynamic cycling of gases [87]. Examples of 'cryogen-free' cooling solutions for SPD platforms are shown in Figure 3. In most cases, cryocoolers use high purity ^{4}He gas that is cycled around a thermodynamic cycle based on the Stirling cycle via mechanical or acoustic compression. The gas is compressed at room temperature, precooled in a heat exchanger and expanded at lower temperature. The low-pressure gas is then passed through the heat exchanger to precool the high-pressure gas before entering the compressor intake. The cycle is then repeated continuously to maintain the base temperature of operation. It is relatively easy to achieve the temperature of operation for SNSPDs ($T \sim 2.5$ K) in a compact system using a two stage Gifford-McMahon (GM) or Pulse Tube (PT) system [88]. Hybrid coolers, such as Joule-Thomson (JT) and Stirling coolers have also been employed [89, 87]. Several commercial solutions using this technology are available in form of turn-key systems, with moderately reduced footprint, that can operate continuously for tens of thousands of hours with little or no maintenance. For a compact GM cooler, the typical compressor power consumption is 1 kW with an air-cooled compressor. If temperatures lower than 1 K have to be reached and stably maintained, like in the case of SNSPDs using lower T_c materials (MoSi and WSi) or for STJ, TES and nano HEB single photon sensors, more sophisticated cryogenic systems using either ^{3}He gas isotope (sorption or dilution refrigerators) or magnetocaloric materials (adiabatic demagnetisation refrigerators - ADRs) have to be used.

Sorption cooling is a kind of refrigeration technology that uses an evaporative cooling principle and it has the advantages of simple design and convenient operation. The main parts are represented by a cryopump (sorption pump), pump tube, condenser, evaporator, gas-gap heat switch, heater and heat sink [90]. When the saturated vapour pressure of refrigerant gas is smaller or ~ 0.005 mbar, the temperatures of ~ 300 mK and ~ 700 mK can be reached if ^{3}He or ^{4}He gases are used respectively. The sorption cooler can be used to provide a low temperature of 300 mK or it can be used as an intermediate stage to provide temperature lower than 1 K heat sink for either adiabatic demagnetisation refrigerators or dilution refrigerators. Single-stage helium sorption coolers were widely used with a superfluid ^{4}He tank as the heat sink in astronomical applications but limited hold times and the rapid development of cryogenic detector technology with higher cooling requirements prompted the development of multistage sorption coolers [91]. This configuration extends holding times and increases the thermal efficiency of the end stage to over 95%. Continuous cooling at 300 mK can be achieved by alternating the operation of twin ^{4}He/^{3}He stages [92 - 94].

Dilution refrigerators use a mixture of ^{3}He/^{4}He gas isotopes and exploit the enthalpy of phase separation of the two gas isotopes to provide continuous cooling ideally down to temperatures as low as 2 mK, with no moving parts in the low-temperature region [95]. These refrigerators need a pre-cooling stage to cool down the ^{3}He gas down to T ~ 1 K that that can be provided either by liquid He (‘wet’ dilution refrigerator) or by aforementioned closed-cycle cryocooling stages (‘dry’ dilution refrigerator). Modern dry dilution refrigerators use high cooling power PT or GM pre-cooling stages with no external supply of cryogenic liquids and with operation that can be highly automated. The main commercial development trend for dry dilution refrigerators is towards larger platforms delivering tremendous cooling power (e.g. for superconducting quantum computing) but compact dry dilution refrigerators have been successfully demonstrated [96]. In ADRs, instead, cooling is obtained by cycling strong magnetic fields in materials such as gadolinium or Ni alloys or paramagnetic salts such as cerium magnesium nitrate in adiabatic cycles to control their entropy [97]. A decrease in the strength of an externally applied magnetic field allows the magnetic domains of the material to become disoriented by action of the thermal energy and if the material is isolated (i.e., an adiabatic process) the temperature drops as the domains absorb the thermal energy to perform their reorientation. Also in this scheme, the precooling is commonly provided from a closed-cycle GM or PT cryocooler for highly automated operation and to avoid external supply of cryogenic liquids.

Despite the unrivalled performance of SPDs, the overall size, weight and power (SWaP) of the cryogenic set up required for their operation is arguably the major obstacle to their wider adoption outside of scientific research. SNSPDs have been demonstrated in space-qualified cooling platforms (e.g. [89]) combining a Stirling JT platform at 4.5 K (cooling technology originally developed for the ESA Planck instrument). There is considerable scope for miniaturisation of chip-based [98, 99] or on-chip [100, 94] and applying these innovative techniques to SPDs. This will open the pathway to wider adoption and deployment of SPDs in challenging remote sensing and advanced imaging applications as part of more complex scientific instruments, or deployed in vehicles, aircraft or satellites.

(a) (b) (c) (d)

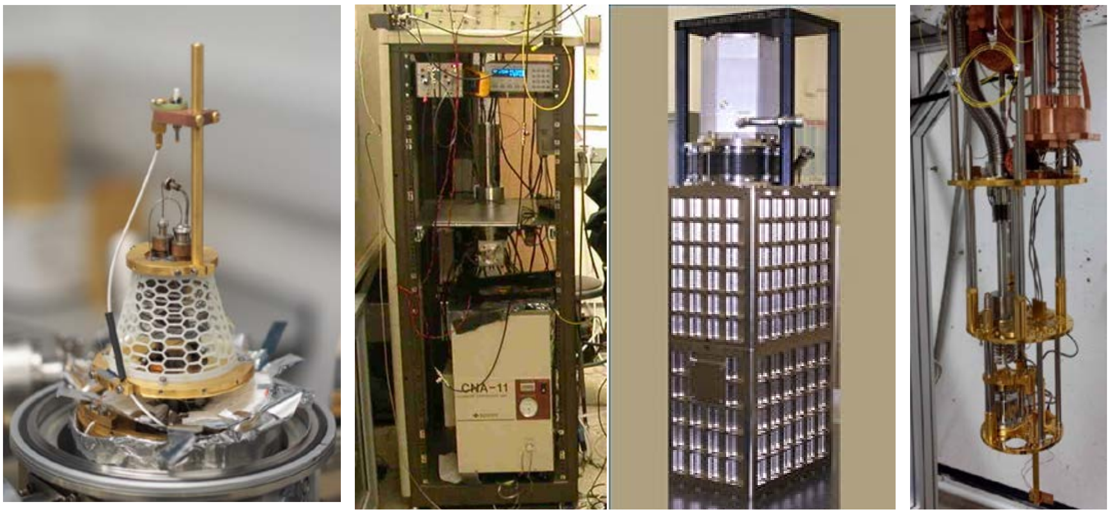

Figure 3. (a) Stirling Joule-Thomson cooler for SNSPD, STFC Rutherford Appleton Laboratory & University of Glasgow, UK, as demonstrated in [89]; (b) Gifford - McMahon cooler for SNSPD, NIST, USA, as employed in [88]; (c) Adiabatic demagnetisation refrigerators for TES, NIST, USA (courtesy of Dr S Nam, Dr A Lita), as employed in [70]; (d) Dilution refrigerator for TES, ALPS, DESY, Germany (courtesy of Dr A Lindner, Dr K-S Isleif) as employed in [101, 102].

3. Detector case studies

In this section we discuss case studies of the major SPD types: STJs (3.1) TESs (3.2), SNSPDs (3.3), KIDs (3.4) and HEBs (3.5). We place particular emphasis on selection and optimisation of suitable SPDs for important applications at infrared wavelengths. This section builds upon our earlier discussion of photon absorption process and detector physics (2.3), superconducting materials (2.4) and cryogenics (2.5).

3.1 Superconducting tunnel junction

The superconducting tunnel junction (STJ) detector relies on the effect of tunnelling of quasiparticles created by photon absorption. STJs are intrinsically fast and capable of resolving the energy of incoming photons. These detectors are successfully used as spectrometers with high resolution and high-count rate capabilities.

The effect of tunnelling of charge carriers through a thin insulating layer forms the basis of a family of light detecting technologies. A superconducting tunnel junction is formed by two superconducting electrodes with a thin layer of insulator between them as shown on figure 3 (a). An incident photon with energy higher than superconducting gap Δ creates excess quasiparticles, which can tunnel through the barrier creating excess current. Number of excess quasiparticles and amplitude of a current pulse is directly proportional to the energy of the absorbed photon. A bias voltage ($V_b < 2\Delta/e$) applied across the junction ensures that the tunnelling process is limited to that involving a transfer of quasiparticles from one superconductor to another as shown on figure 3 (b). To suppress the tunnelling of Cooper pairs the small magnetic field is usually applied in parallel to the junction. The theoretically achievable energy resolution of an STJ is given by $\Delta E_{\mathrm{FWHM}} = 2.355\sqrt{F\varepsilon h\nu}$, where F is the Fano factor describing the statistical fluctuations of the charge generation, ε is the mean energy required for the creation of quasiparticles and $h\nu$ is the photon energy. For Nb material, $F = 0.22$ and $\varepsilon = 1.7\Delta$ with the factor of 1.7 that accounts for the partial energy loss into the photon system [103, 104]. As STJ detectors have high impedance, they are usually read out with a field-effect transistor (FET) based preamplifier. Total system noise includes contributions from tunnelling and FET preamplifier. Counting of optical and UV photons was demonstrated in [56] where authors achieved spectral resolution of 45 nm with photons in the wavelength range of 200 to 500 nm.

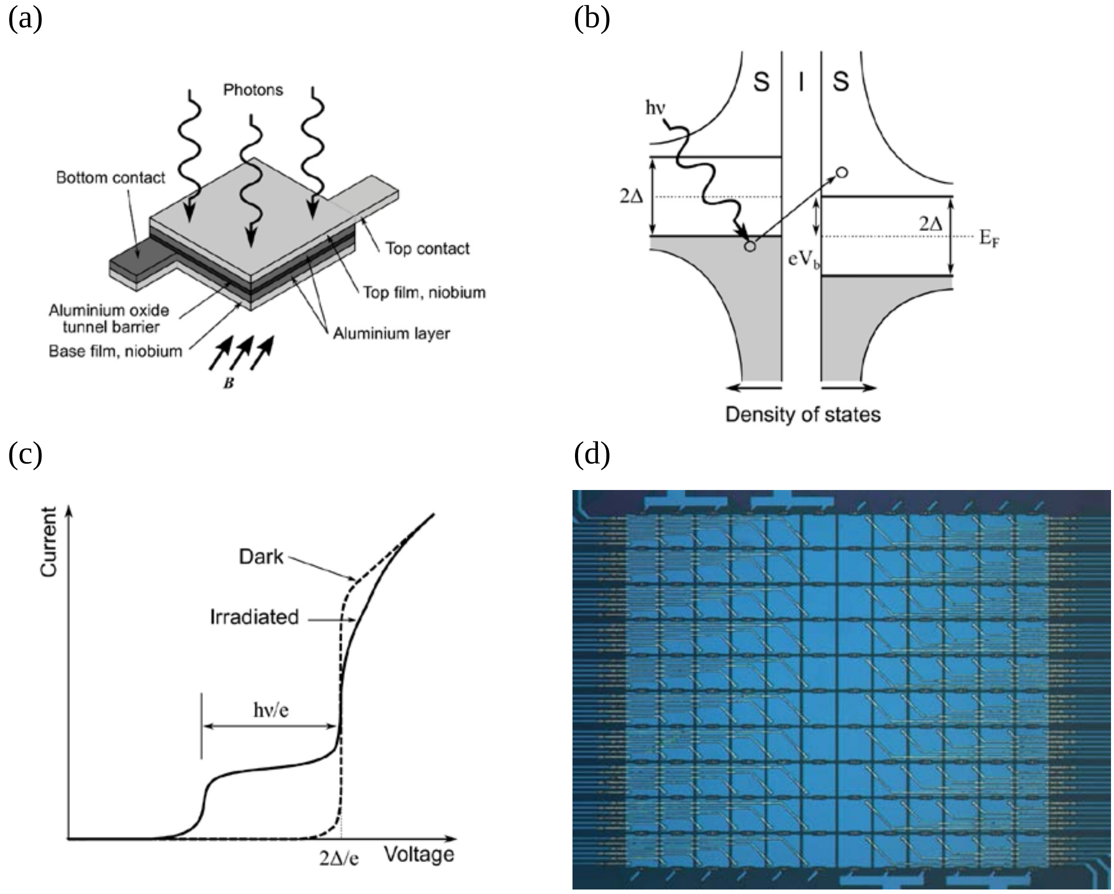

Figure 4. (a) STJ detector of optical photons based on Nb superconductor and Al_2O_3 insulation barrier, adapted from [56]; (b) energy diagram of STJ with applied bias; (c) idealised voltage-current characteristic of an STJ; (d) photo of S-Cam3 array, ESA (Courtesy of Dr D.D.E. Martin and Dr P Verhoeve) [105]. (d) is reproduced with permission from D.D.E. Martin *et al.* Proc SPIE vol 6269 p.238-248 (2006) [105], copyright SPIE publishing 2006.

Other variations of superconducting tunnelling devices include Normal metal – insulator – superconductor junction (NIS) [106, 107] cold electron bolometer (CEB) [108] and superconductor - semiconductor - superconductor bolometer (S-Sm-S) [109, 110]. Applications in optical astronomy have been the main drivers behind the development of STJ detectors. Spectroscopy of faint optical sources is of particular interest, as charged-coupled device (CCD) cameras do not provide any intrinsic energy resolution capability. The European Space Agency (ESA) has operated an optical STJ camera since 1999 with the latest generation named “S-Cam3”. This STJ camera had a 10 × 12 pixel array with an average energy resolution of ΔE_{FWHM} = 0.17 eV at 2.4 eV (λ = 500 nm). The camera covered a band from 340 to 740 nm with peak detection efficiency of 34% at 550 nm and the absolute time of 1 μs [105]. Energy resolution ability of STJ detectors was leveraged to make X-ray spectrometers for synchrotron science [111 - 113]and for plasma and ion physics experiments [73].

There is recent interest in exploiting the giant thermoelectric effect in superconductor-ferromagnet junctions for highly sensitive photon detectors [114, 115]. With recent introduction of new materials such as graphene, the interest in quantum detectors based on junctions has been revived. Bolometers based on superconductor-insulator-graphene junctions have been explored [116]. Recently a graphene-based Josephson junction capable of single-photon detection of near-infrared radiation has been demonstrated [117]. One proposed application is to enable low-power optical interconnects for future architectures of superconducting quantum computers.

3.2 Transition Edge Sensor

The Transition Edge Sensor (TES) exploits the sharp nonlinearity of the superconducting transition to achieve extremely sensitive radiation detection. In the context of infrared single-photon detection, this confers energy resolution, or at fixed photon wavelength, photon number resolution. At optical and near-infrared wavelengths the quantum efficiency of TES detectors is close to unity.

Detectors based on the abrupt change in resistivity at the superconducting transition have been developed into useful technology applicable across many parts of the EM spectrum from THz to X-rays [7, 118, 119]. TES detectors use an absorber to convert photons into heat and superconducting films biased within resistive transition as a sensitive thermometer. Due to the nature of bolometric response, TES detectors can be designed for single photon detection and energy resolution across a wide range of wavelengths including UV, optical and IR. Voltage bias is widely adopted method of the TES operation which takes advantage of negative electro-thermal feedback (ETF) to stabilise the bias point on the superconducting transition and to reduce the effective time constant [118]. A temperature increase due to the deposited photon energy results in a rapid change in the device resistance. The corresponding change in the bias current is then measured with a SQUID amplifier. The absorber and thermometer are coupled to the heat bath through a thermal link. The value of the link's thermal conductance (G) is usually chosen to ensure that the excess heat is removed from the absorber efficiently. In general, TES can be described by the heat balance equation:

$$C(T)\frac{\mathrm{dT}}{\mathrm{dt}} = P_{\mathrm{opt}} + P_{\mathrm{DC}} - \int_{T_{\mathrm{b}}}^{T} G(T)dT,$$

where $C(T)$ is the heat capacity of the absorber and thermometer, P_{opt} is the optical power, P_{DC} is the power of DC bias and the third term is the heat flow through the link in the form $P = k(T_{\mathrm{c}}^{n} - T^{n})$. Thermal conductance equals to $G = \frac{dP}{dT} = knT^{n-1}$. In the small signal approximation, responsivity is proportional to reversed bias voltage (V_{b}): $S = -V_{\mathrm{b}}^{-1} \times \left(\frac{L}{L+1}\right) \times (1 + i\omega\tau)^{-1}$, where $L \equiv \alpha P_{\mathrm{DC}}/GT_{\mathrm{b}}$ [118] is the loop gain and τ is the time constant. The temperature coefficient of resistance is defined as $\alpha = (T/R)(\mathrm{d}R/\mathrm{d}T)$.The time constant of the TES response is also influenced by the ETF as $\tau = \tau_0/(1+L)$ where $\tau_0 = C/G$ is the thermal time constant of the bolometer. TES noise equivalent power without optical load has contributions from Johnson noise, thermal fluctuations (phonon) noise and SQUID amplifier noise. Theoretical performance is given by the phonon noise as $NEP_{\mathrm{phonon}} = \sqrt{\gamma 4 k_{\mathrm{B}} T^{2} G}$, where γ is the factor with the value between 0.1 and 1. Energy resolution of the detector is $\Delta E \approx NEP\sqrt{\tau}$. Single photon TES detectors at optical and infrared wavelengths use tungsten (W) as an absorber and thermometer. In this case, the photon energy is absorbed by electrons in the film and the heat escapes to the bath by means of electron-phonon interaction as $P_{\mathrm{e-ph}} = \Sigma_{\mathrm{e-ph}} A\left(T_{\mathrm{e}}^{5} - T_{\mathrm{b}}^{5}\right)$, where $\Sigma_{\mathrm{e\text{-}ph}}$ is material specific parameter describing e-ph coupling and T_{b} is bath temperature.

(a)

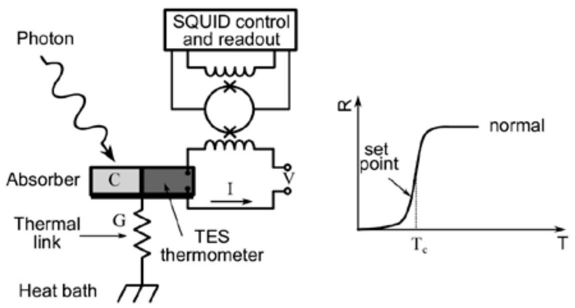

(b)

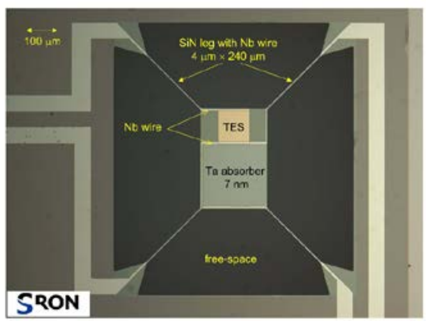

(c)

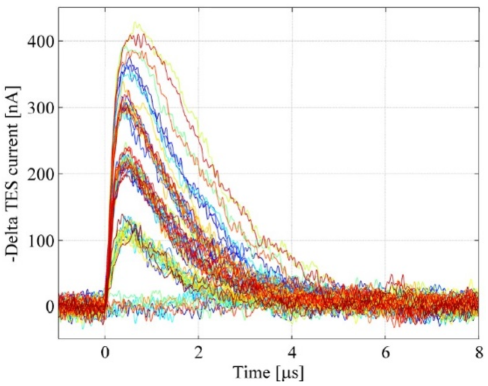

(d)

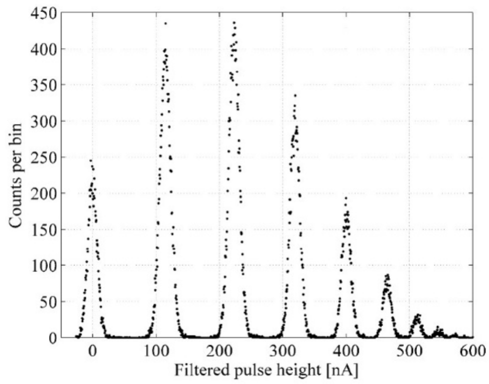

Figure 5. (a) Schematic of transition edge sensor and idealised resistive transition, adapted from [119]; (b) image of SiN suspended TES bolometer, SRON (courtesy of Dr J Gao) [120]; (c) and (d) multi-photon response of the TES (courtesy of Dr A. Lita) [74]. (b) is reproduced with permission from D. Morozov *et al.* IEEE Trans. Appl. Supercond. vol 21 p.188-191 (2011) copyright IEEE publishing (2011) [120]. (c) and (d) are reproduced with permission from A. Lita *et al.* Proc SPIE vol. 7681 p. 71-80 (2010) copyright SPIE publishing 2010 [74].

State of the art optical TES detectors employing an optical cavity design have shown ~98% quantum efficiency at 850 nm [58] and 95% at 1550 nm [70, 74]. At the same time, the reported timing resolution (jitter) is few microseconds. In contrast to “clicking” photon detectors, TES devices are intrinsically capable of photon number resolution (PNR). Typical response of the TES to a few photon pulses is shown on Figure 5 (c). High efficiency coupled with PNR capability makes optical and infrared TES detectors an attractive technology for applications in a wide range of groundbreaking quantum optics experiments [121], such as the Hong-Ou-Mandel experiment [122]; fundamental tests of quantum non-locality [123] and loophole free test of Bell’s inequality [124]; measuring optical power over high dynamic range down to the few photon level [121, 125]. Quite recently, Boson sampling approaches to optical quantum computing have been advanced by deployment of TES detectors [126]. TES detectors are also a key enabling technology in the search for Dark Matter. The Any Light Particle (ALPS II) experiment at DESY relies on TES devices to detect the 1064 nm photon produced due to creation and annihilation of an axion in the ‘light shining through the wall’ experiment [101, 102]. Importantly for the development of large-scale instrumentation, TES detectors can be multiplexed in the time- or frequency domain reaching few kilo-pixels scale [127, 128].

3.3 Superconducting Nanowire Single Photon Detector

Superconducting nanowire single photon detectors (SNSPDs) offer high speed, low noise and high efficiency single photon detection from UV to mid infrared wavelengths at an operating temperature of 0.8 K or above.

The concept of the superconducting nanowire single photon detector (known as SSPD or SNSPD) in the literature was introduced and demonstrated by Gregory Gol'tsman and co-workers in 2001 [63]. The basic SNSPD device is a narrow wire defined in an ultrathin superconducting thin film (originally niobium nitride). The device is cooled below the superconducting transition temperature and current-biased just below the superconducting critical current. In this state, a single infrared photon can switch the SNSPD from the superconducting to the resistive state. This triggers a fast voltage pulse which can be readily amplified and read out with room temperature electronics. SNSPDs operate in the temperature range 0.8 - 4 K making them accessible with liquid helium or affordable closed-cycle cooling. The timing jitter of the SNSPD (uncertainty between photon arrival and readout electrical pulse) is exceptionally low. Understanding of the hotspot formation and relaxation mechanism has improved with theoretical developments [67, 129 - 131]. With careful engineering of the microwave waveguide surrounding the nanowire [69] timing jitter as low as 3 ps FWHM has been demonstrated – the time it takes a photon in free space to travel 1 millimetre.

The most established SNSPD material is niobium nitride (NbN) [6], with NbTiN [132] a common alternative. NbN has short thermal time constants for hot electron and phonon relaxation processes [133]. Other superconducting transition metal nitrides have been explored (TaN) [134], MoN [135] with some marginal advantages claimed. Pure metallic superconductors (Nb) do not allow the correct balance between hotspot growth following photon absorption due to Joule heating and rapid heat dissipation [136]. A significant advance has been the adoption of amorphous superconductors WSi [137] and MoSi [138], which allowed saturated behaviour of photon detection probability versus bias current to be more easily obtained, enabling near unity efficiency [68, 139] and improving device yield even over large areas. The most common deposition method is sputtering, but new techniques such as atomic layer deposition are showing promise [140]. Higher transition temperature superconducting materials have been explored.

Magnesium diboride MgB_2 SNSPDs have shown single photon sensitivity up to 1550 nm [141], but uniformity and yield is a significant problem. YBCO SNSPDs have been attempted [142] and recent studies have targeted BSCCO [143]. Bolometric behaviour has been observed in few layer $NbSe_2$ operated under current bias [144].

The canonical SNSPD has two drawbacks: the nanowire cross-section is minute and the ultrathin superconducting material is semitransparent. The main approach to increasing the cross-section (e.g. for optical coupling with single-mode optical fibre) is to scale up to a meander design [145]. The absorption can be enhanced by embedding the SNSPD into an optical cavity [146]. High efficiency at near IR has been achieved by many groups [147 - 150]. Record results are 93% with WSi [139] and 98% with MoSi [68] at 1550 nm. Other photonic design strategies can also be employed to enhance optical coupling to the nanowire and photon absorption, including nanoantenna designs [151, 152] and waveguide integration [153 - 157].

(a) (b)

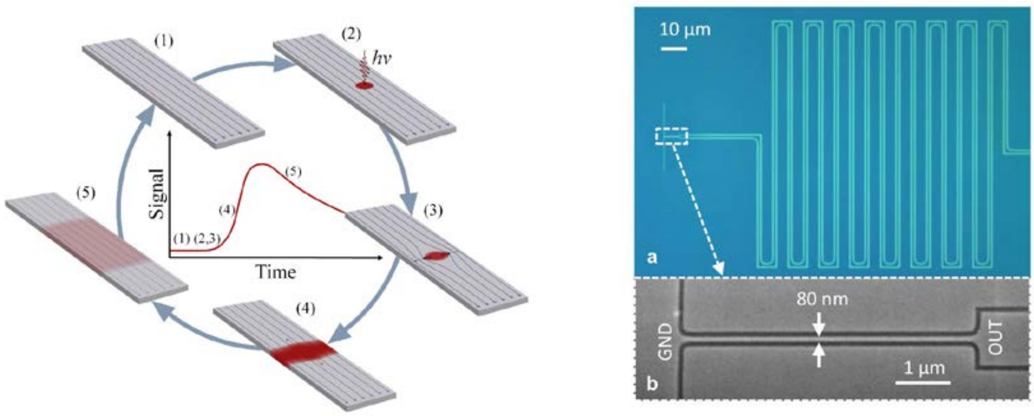

Figure 6. (a) SNSPD mechanism of response (courtesy of Dr J Allmaras) [158]; (b) micrographs of an ultra-low timing jitter SNSPD device (courtesy of Dr B Korzh) [69]. (a) and (b) are reproduced with permission from R. H. Hadfield Nat. Photon vol. 14 p.201-202 (2020) [158] copyright Springer Nature 2020.

In the past decade there has been increasing interest in scaling up from single-pixel SNSPDs to large area arrays [10]. Several challenges present themselves: nanowire device yield over large areas and efficient readout without unfeasible wiring. The yield issue has been mitigated by the advent of more uniform amorphous superconducting materials. A number of promising multiplexing schemes [159] have been proposed and demonstrated: row-column readout [160, 161], single flux quantum logic readout [162-

164], RF readout [165] and optical modulator readout [166]. A recent landmark result has been a kilopixel array of SNSPDs with row-column readout [167]. SNSPD development has been pursued by academic groups, major national laboratories and increasingly, commerical companies. There is considerable appetite from end-users for high performance infrared photon counters such as SNSPDs, particularly if supplied in turnkey, closed-cycle cryogenic systems (Section 2.5). High quality systems for laboratory-based applications are in widespread use. There is clear potential for miniaturisation of the cryogenic hardware if major industrial players seize the opportunity [89]. The end-user interest is spurred by usefulness of SNSPDs in infrared time-correlated single-photon counting (TCSPC) scenarios. Applications for SNSPDs span communications, computing, spectroscopy, remote sensing. In terms of communications, long distance quantum key distribution in optical fibre was a breakthrough application for SNSPDs [168 - 174]. SNSPDs have also been an essential tool in the development of quantum networks with remotely entangled qubits [175 - 178]. SNSPDs have also been employed in receivers for space-to-ground classical communications such as the NASA 2014 LADEE Lunar Laser Communications (LLCD) demonstration [179]. SNSPDs are expected to be deployed for the upcoming NASA Deep Space Optical Communications (DSOC) mission [180] and are under consideration for futuristic proposals such as Breakthrough Starshot [181]. Waveguide integrated SNSPDs [153 - 155] offer a scalable platform for photonic computing with single photon signals. There is a route to the realisation of optical quantum computing [182 - 184]. Optical neuromorphic computing can exploit similar SNSPD architectures [185]. SNSPDs lend themselves very well to TCSPC spectroscopy, of emitters such as semiconductor quantum dots [88], singlet oxygen luminescence [186] and even sensing the atmospheres of exoplanets [37]. The ultra-low dark counts of the latest SNSPDs makes them a valuable tool in low mass/energy Dark Matter searches [187, 188]. With excellent timing resolution there is considerable potential for deployment of SNSPDs in remote sensing. Via optical fibre, SNSPDs lend themselves to optical time domain reflectrometry [189] and recently have been employed as a central component of the ESA Ariane 6 rocket launch system [190]. Fibre Raman Temperature sensing with SNSPDs has also been demonstrated with SNSPDs [191, 192] and could be extended to applications such as geothermal energy. In free space SNSPDs have been employed in daylight single photon LIDAR at 1550 nm [193, 194] and proof of principle demonstrations have been carried out at 2.3 μm [195].

3.3 Kinetic Inductance Detectors

Microwave kinetic inductance detectors (KIDs or MKIDs) exploit the change in kinetic inductance of a superconducting resonator upon absorption of photons, shifting the resonant frequency in the microwave regime. Multiple KID pixels can be embedded in a single microwave coplanar waveguide, each tuned to an individual readout frequency. In this way KIDs are well-suited for multiplexing in large scale arrays. KIDs are able to measure the energy of absorbed photons, which in turn confers the ability to detect multi-photon states.

The typical KID device consists of a superconducting strip cooled down well below the T_c and forming an active part of a resonant circuit. The detection mechanism is based on the change of kinetic inductance L_k of the superconductor due to generation of quasiparticles by incident electro-magnetic radiation. The change in L_k is then measured as a change of amplitude or a phase of the microwave signal transmitted through a circuit. Reading out KID pixels with high quality factor resonant circuits can allow frequency-domain multiplexing of thousands of resonators through a single coaxial cable and a single HEMT amplifier [60]. Another advantage of KIDs is the relative simplicity of fabrication. In many cases fabrication of the full array requires only one lithographic step.

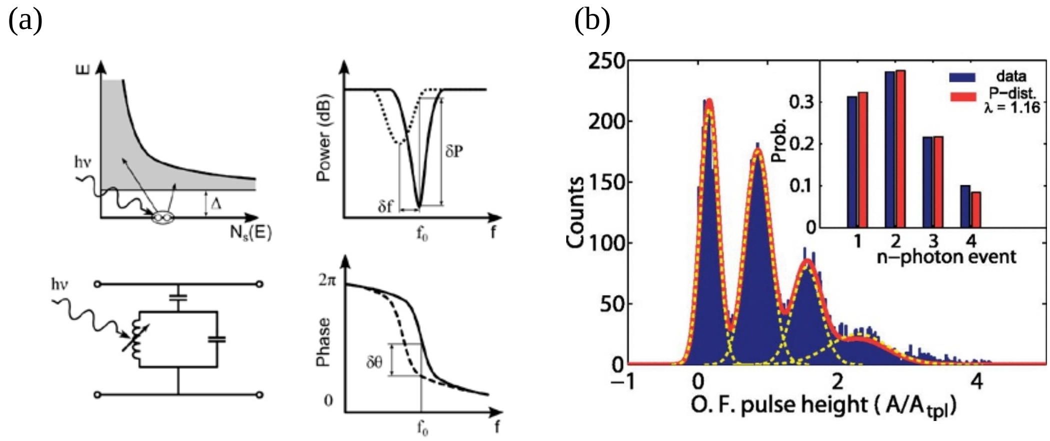

(c)

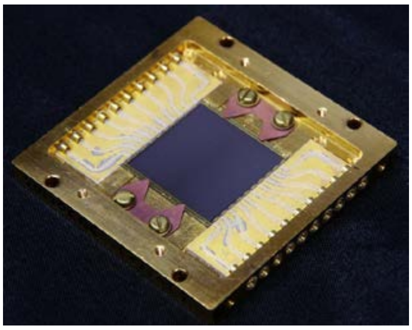

Figure 7. (a) Kinetic Inductance Detector (photon absorption, resonant circuit, and the idealised illustration of the resonance frequency and phase shift), adapted from [60], (courtesy of Dr P Day); (b) response of TiN MKID to 1550 nm photons [61]; (c) 140×146-pixel near-IR MKID array (courtesy of Prof B Mazin) [196]. (b) is reproduced with permission from J. Gao *et al.* Applied Physics Letters vol. 101 p. 142602 (2012) [61] copyright AIP publishing 2012. (c) is reproduced with permission from P. Szypryt *et al*. Opt. Express vol. 25 p. 25894-25909 (2017) [196] © The Optical Society.

The fundamental noise limit of a KID is set by quasiparticle generation-recombination noise and is given by $NEP_{GR}^2 = 4\Delta^2(N_{qp}/\tau_{qp})$ [197], where the number of quasiparticles is N_{qp}, τ_{qp} is the quasiparticle lifetime and Δ is the energy gap of the superconductor. In theory, $NEP \sim 10^{-20}$ $\mathrm{W}/\sqrt{\mathrm{Hz}}$ might be possible in an extreme situation with low number of quasiparticles $N_{qp} \sim 100$ and $\tau_{qp} \sim 10$ ms. In practice, $NEP \approx 4\times10^{-19}$ $\mathrm{W}/\sqrt{\mathrm{Hz}}$ has been derived from the noise measurements in the lab environment [198] and recent measurements of $N_{qp} \approx 30000$ and $\tau_{qp} \sim 20$ ms in KID fabricated out of Al film also suggest $NEP_{GR} = 2\times10^{-19}$ $\mathrm{W}/\sqrt{\mathrm{Hz}}$ measured at the temperatures below 180 mK [199]. At first, KIDs were designed for THz detection in astronomy [200] and adapted to passive THz imaging [62]. Owing to ease of multiplexing and fabrication, this technology has been expanded to other parts of EM spectrum including optical and infrared. Large arrays of few kilo-pixels were developed and used on optical and infrared astronomical telescopes (Figure 7(c)) [196, 83]. An early demonstration of single photon detection with TiN MKID was made by Gao *et al.* [61]. MKID based on TiN film has shown energy resolution of $\Delta E = 0.27$ eV when detecting 1550 nm photons (Figure 7 (b)). Recently PtSi and Al based MKIDs were shown to have a single photon response in optical and infrared [201 - 203].

3.5 Hot Electron Bolometers

The superconducting Hot Electron Bolometer (HEB) exploits the strong dependence of the resistance on electron temperature and is based on electron heating by external radiation. HEB detectors are extremely fast due to the rapid nature of electron energy relaxation and are intrinsically capable of energy resolution.

HEBs were first based on semiconducting materials with strong temperature dependence of resistance, such as InSb [204, 205]. In the early1990s, E. M. Gershenzon *et al*. demostrated an HEB based on a thin superconducting Nb film [206, 207]. The device utilised the hot electron effect in a thin superconducting film (typically a refractory metal or nitride e.g. Nb, NbN, Al, Ti etc). In general, a hot electron model applies to superconductors in the resistive state just below T_c. In this state electrons and phonons can be described by thermal distribution functions with effective temperature for each subsystem. The effective temperature of the electron system (T_e) and effective temperature of phonons (T_{ph}) are assumed to be uniform throughout the detector. This means that the thermalisation times inside each subsystem (τ_{th} for the electrons and $\tau_{ph\text{-}ph}$ for the phonons) are much shorter than the time of energy exchange between subsystems ($\tau_{e\text{-}ph}$). Incoming EM radiation is absorbed directly by electrons and elevates T_e above bath temperature. Depending on the size of the device, energy relaxation of hot electrons can rely either on emission of the phonons with characteristic time $\tau_{e\text{-}ph}$ or on diffusion of the hot electrons into contacts with characteristic time $\tau_{diff} = L^2/(\pi^2 D)$, where L is the device length and D is the electron diffusion constant. The first mechanism ("phonon cooling") takes place in relatively large devices with $L > L_{\mathrm{diff}} = \sqrt{D\,\tau_{\mathrm{e-ph}}}$. The second mechanism ("diffusion cooling") takes place with $L < L_{\mathrm{diff}}$. Both mechanisms can coexist and the dominance of one over another depends on the HEB size, the choice of material and the operating temperature [208, 209]. Resistance of the detector near T_c rapidly depends on T_e allowing measurement of EM radiation power by registering the change in resistance. Due to their small size HEB detectors rely on planar antenna to couple to radiation and employ low noise FET amplifiers for the readout. Owing to their fast relaxation times, HEBs are widely used as THz mixers with the intermediate frequency bandwidth of a few GHz.

The intrinsic noise of a HEB consists of thermal energy fluctuation (TEF) or phonon noise and Johnson noise. Phonon noise plays significant role and depends on T_e

and $G_{\text{e-ph}}$ as $NEP_{\text{TEF}} = \sqrt{\xi k_{\text{B}} T_{\text{e}} G_{\text{e-ph}}}$, where ξ = 4 for $T_{\text{e}} = T$, and ξ = 2 for $T_{\text{e}} >> T$ [210]. Both $G_{\text{e-ph}}$ and NEP_{TEF} can be reduced by reducing the HEB volume. The time constant $\tau_{\text{e-ph}} = C_{\text{e}}/G_{\text{e-ph}}$. can be controlled by choosing superconducting materials with strong electron-phonon coupling such as NbN and by decreasing the film thickness such as emitted photons can escape to the substrate rather than be reabsorbed by the electrons. Ultra-low $NEP = 3\times10^{-19}$ W/$\sqrt{\text{Hz}}$ was achieved for Ti based HEB (Figure 8 (a)) in the far infrared wavelength band with potential capability close to 10^{-20} W/$\sqrt{\text{Hz}}$ [72].

(a) (b)

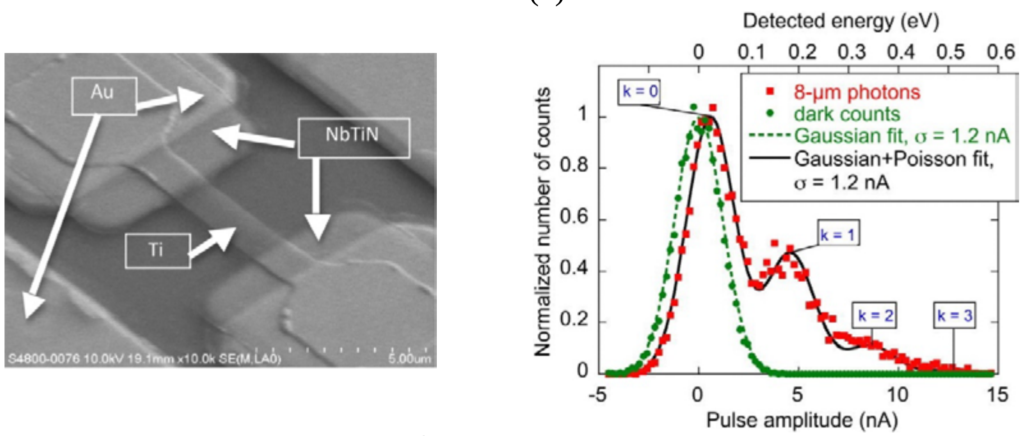

Figure 8. (a) SEM image of 1×2 μm^2 HEB device (courtesy of Dr B Karasik) [72] ; (b) detection of single 8 μm photons [211]. (a) is reproduced with permission from B.S.Karasik *et al.* IEEE Trans. Terahertz Science & Technology vol 1 pp. 97-111 (2011) [72] copyright IEEE 2011. (b) is reproduced with permission from B.S.Karasik *et al.* Applied Physics Letters vol. 101 p.052601 (2012) [211] copyright AIP Publishing.

A similar nano-scale Ti HEB device (Figure 8 (a)) with SQUID readout has demonstrated mid infrared single photon detection capability at λ = 8 μm with energy resolution ΔE_{FWHM} = 0.11 eV [211]. It has been shown that HEBs can be integrated with optical waveguides at 1550 nm for quantum optics applications [212] and they are compatible with other SPD technologies such as SNSPDs, providing a potentially very useful combination of heterodyne detection and fast photon counting in quantum optics and other quantum technologies.

4. Conclusion and Outlook

In this review we have presented the background of superconducting photon detectors (SPDs), with particular emphasis on photon detection at visible and infrared wavelengths. We have surveyed the current state-of-the-art across the leading SPD technologies: superconducting tunnel junctions (STJs), transition edge sensors (TESs), superconducting nanowire single-photon detectors (SSPDs or SNSPDs), kinetic inductance detectors (KIDs) and hot electron bolometers (HEBs). These are the main SPD types which at the time of writing have made it through the demanding process of technological selection. These mature SPDs concepts have been trialled and adopted in important photon counting applications and scaled up to large arrays of high-performance pixels.

SPDs have been considered for at least half a century. Forecasting the future long term technological development path over the next half century is notoriously challenging. However, we can confidently predict SPDs will remain an important area of development in applied physics and source of exciting new technologies for the most demanding scientific applications. Firstly, superconducting phenomena are observed across a tremendous variety of elements and compounds. High temperature superconductors have not yet had the hoped-for impact in terms of SPDs, but new candidate materials and processing techniques are frequently being brought forward. The huge research effort stimulated by the discovery of graphene has brought two dimensional superconducting materials (e.g. $NbSe_2$) into consideration. Twisted bilayer or 'magic angle' graphene exhibits superconducting properties and has been demonstrated in devices. The burgeoning field of superconducting qubits for quantum computing (now a multi-billion-dollar industry) benefited from expertise and techniques used in SPDs. This is progressing towards cryogenic data centres and interconnected superconducting quantum computers – SPDs would naturally dovetail as a useful compatible technology for low energy optical interconnects. Effectively these advanced superconducting quantum circuits are manipulating and detecting single photons at microwave wavelengths. Researchers have naturally foreseen the potential of the advanced toolkit of superconducting qubits for low energy photon detection and also the detection of dark matter and exotic fundamental particles (e.g. anyons). We have surveyed the role SPDs (especially SNSPDs) have played in opening up infrared photon counting in areas such as quantum communication, remote sensing and life sciences, and have been commercialised for R&D markets. As highlighted in section 2.5, the wider adoption of emerging SPD technology as a standard tool (e.g. in single photon LIDAR systems or fluorescence microscopy) depends on cost, size weight and power considerations – if compact, reliable, turnkey high performance SPD systems can be offered at affordable prices the customers will adopt the technology. In this commercial arena investment in cryogenic engineering is likely as important as future development in the device technologies themselves. Looking at the 50-year horizon, the most demanding frontier for new technologies is arguably space. Space-based astronomy is entering a new era with the launch of the James Webb Space Telescope (launched in December 2021) and networks of satellites ring the earth and are likely to be extended across the solar system. The costs of launching space-borne instrumentation and satellites are dropping. Superconducting devices are more durable than CMOS in the harsh environment of space. There is a likely demand for SPDs in next generation instrumentation for exoplanet searches and the search for alien life, and in deep space optical communications at the single photon limit. We are certain this review is only the most recent chapter in the overall development of SPD technology.

Acknowledgements

The authors thank the Editor Professor Sir Peter Knight for the kind invitation to prepare this topical review. The authors acknowledge support from the UK National Quantum Technology Programme (EP/S026428/1, EP/T001011/1, EP/T0097X/1, ST/T005920/1). The authors are grateful to expert colleagues across the world for giving permission for their work to be included in this topical review. The authors thank Dr Gregor Taylor for useful comments on the final manuscript.

References

[1] P. L. Richards, "Bolometers for infrared and millimeter waves," *J. App. Phys.*, vol. 76, pp. 1-24, July 1994.

[2] C. Silberhorn, "Detecting quantum light," *Contemporary Physics*, vol. 48, pp. 143-156, 2007.

[3] R. H. Hadfield, "Single-photon detectors for optical quantum information applications," *Nat Photon*, vol. 3, p. 696–705, December 2009.

[4] M. D. Eisaman, J. Fan, A. Migdall and S. V. Polyakov, "Invited Review Article: Single-photon sources and detectors," *Review of Scientific Instruments,* vol. 82, p. 071101, 2011.

[5] C. M. Natarajan, M. G. Tanner and R. H. Hadfield, "Superconducting nanowire single-photon detectors: physics and applications," *Superconductor Science and Technology,* vol. 25, p. 063001, 2012.

[6] I. Holzman and Y. Ivry, "Superconducting Nanowires for Single-Photon Detection: Progress, Challenges, and Opportunities," *Advanced Quantum Technologies,* vol. 2, p. 1800058, 2019.

[7] J. N. Ullom and D. A. Bennett, "Review of superconducting transition-edge sensors for x-ray and gamma-ray spectroscopy," *Superconductor Science and Technology,* vol. 28, p. 084003, July 2015.

[8] J. Zmuidzinas and P. L. Richards, "Superconducting detectors and mixers for millimeter and submillimeter astrophysics," *Proceedings of the IEEE,* vol. 92, pp. 1597-1616, October 2004.

[9] J. Zmuidzinas, "Superconducting Microresonators: Physics and Applications," *Annual Review of Condensed Matter Physics,* vol. 3, pp. 169-214, 2012.

[10] S. Steinhauer, S. Gyger and V. Zwiller, "Progress on large-scale superconducting nanowire single-photon detectors," *Applied Physics Letters,* vol. 118, p. 100501, 2021.

[11] I. E. Zadeh, J. Chang, J. W. N. Los, S. Gyger, A. W. Elshaari, S. Steinhauer, S. N. Dorenbos and V. Zwiller, "Superconducting nanowire single-photon detectors: A perspective on evolution, state-of-the-art, future developments, and applications," *Applied Physics Letters,* vol. 118, p. 190502, 2021.

[12] A. Smith, "Selected papers on photon-counting detectors," *SPIE milestone series*, vol. MS 143, 1998.

[13] A. Migdall, S. V. Polyakov, J. Fan and J. C. Bienfang, Eds., “Single-Photon Generation and Detection,” in *Single-Photon Generation and Detection*, vol. 45, Academic Press, 2013, p. iii.

[14] R. H. Hadfield and G. Johansson, Eds., Superconducting Devices in Quantum Optics, 1 ed., Springer International Publishing, 2016, pp. XIII, 249.

[15] N. E. Booth and D. J. Goldie, “Superconducting particle detectors,” *Superconductor Science and Technology*, vol. 9, p. 493–516, July 1996.

[16] D. Twerenbold, “Cryogenic particle detectors,” *Reports on Progress in Physics*, vol. 59, p. 349–426, March 1996.

[17] G. N. Lewis, “The Conservation of Photons,” *Nature*, vol. 118, p. 874–875, 1926. See also APS News 21, 11 December 2012

[18] C. Cohen-Tannoudji, J. Dupont-Roc and G. Grynberg, Photons and Atoms - Introduction to Quantum Electrodynamics, 1997.

[19] R. Loudon, The Quantum Theory of Light, 3 ed., p. 448.

[20] M. Planck and M. Masius, The theory of heat radiation, Philadelphia, P. Blakiston's Son & Co., 1914.

[21] M. Planck, *Verhandl. Dtsch. phys. Ges.*, vol. 2, p. 202, 1900.

[22] D. Ter Haar, The Old Quantum Theory, Pergamon, 1967.

[23] A. Einstein, *Annalen der Physik*, vol. 17, pp. 132-147, 1905.

[24] A. B. Arons and M. B. Peppard, “Einstein's Proposal of the Photon Concept—a Translation of the Annalen der Physik Paper of 1905,” *American Journal of Physics,* vol. 33, pp. 367-374, 1965.

[25] A. H. Compton, “The Spectrum of Scattered X-Rays,” *Phys. Rev.*, vol. 22, no. 5, p. 409–413, November 1923.

[26] *Technical Report on Quantum Cryptography Technology Experts Panel, ARDA - see http://qist.lanl.gov/,* 2004.

[27] A. Ekert, N. Gisin, B. Huttner, H. Inamori and H. Weinfurter, “Quantum Cryptography,” in *The Physics of Quantum Information: Quantum Cryptography, Quantum Teleportation, Quantum Computation*, D. Bouwmeester, A. Ekert and A. Zeilinger, Eds., Berlin, Heidelberg: Springer Berlin Heidelberg, 2000, p. 15–48.

[28] T. Isoshima, Y. Isojima, K. Hakomori, K. Kikuchi, K. Nagai and H. Nakagawa, “Ultrahigh sensitivity single-photon detector using a Si avalanche photodiode for the measurement of ultraweak biochemiluminescence,” *Review of Scientific Instruments,* vol. 66, pp. 2922-2926, 1995.

[29] J.-P. Knemeyer, N. Marmé and M. Sauer, “Probes for Detection of Specific DNA Sequences at the Single-Molecule Level,” *Anal. Chem.*, vol. 72, p. 3717–3724, August 2000.

[30] S. Weiss, “Fluorescence Spectroscopy of Single Biomolecules,” *Science,* vol. 283, no. 5408, pp. 1676-1683, 12 March 1999.

[31] D. A. Boas, D. H. Brooks, E. L. Miller, C. A. DiMarzio, M. Kilmer, R. J. Gaudette and Q. Zhang, “Imaging the body with diffuse optical tomography,” *IEEE Signal Processing Magazine,* vol. 18, pp. 57-75, 2001.

[32] M. T. Jarvi, M. J. Niedre, M. S. Patterson and B. C. Wilson, "Singlet Oxygen Luminescence Dosimetry (SOLD) for Photodynamic Therapy: Current Status, Challenges and Future Prospects," *Photochemistry and Photobiology,* vol. 82, pp. 1198-1210, 2006.

[33] M. Viterbini, A. Adriani and G. Di Donfrancesco, "Single photon detection and timing system for a Lidar experiment," *Review of Scientific Instruments,* vol. 58, pp. 1833-1839, 1987.

[34] M. Legré, R. Thew, H. Zbinden and N. Gisin, "High resolution optical time domain reflectometer based on 1.55μm up-conversion photon-counting module," *Opt. Express,* vol. 15, p. 8237–8242, June 2007.

[35] H. Hemmati, A. Biswas and I. B. Djordjevic, "Deep-Space Optical Communications: Future Perspectives and Applications," *Proceedings of the IEEE,* vol. 99, pp. 2020-2039, 2011.

[36] F. Stellari, A. Tosi, F. Zappa and S. Cova, "CMOS circuit testing via time-resolved luminescence measurements and simulations," *IEEE Transactions on Instrumentation and Measurement,* vol. 53, pp. 163-169, 2004.

[37] V. B. Verma, B. Korzh, A. B. Walter, A. E. Lita, R. M. Briggs, M. Colangelo, Y. Zhai, E. E. Wollman, A. D. Beyer, J. P. Allmaras, H. Vora, D. Zhu, E. Schmidt, A. G. Kozorezov, K. K. Berggren, R. P. Mirin, S. W. Nam and M. D. Shaw, "Single-photon detection in the mid-infrared up to 10 μm wavelength using tungsten silicide superconducting nanowire detectors," *APL Photonics,* vol. 6, p. 056101, 2021.

[38] H. K. Onnes, *Commun. Phys. Lab Univ. Leiden. Suppl.,* vol. 29, 1911.

[39] W. Meissner and R. Ochsenfeld, *Naturwissenschaften,* vol. 21, p. 787, 1933.

[40] F. London, “On the Problem of the Molecular Theory of Superconductivity,” *Phys. Rev.,* vol. 74, no. 5, p. 562–573, September 1948.

[41] V. L. Ginzburg and L. D. Landau, “On the Theory of superconductivity,” *Zh. Eksp. Teor. Fiz.,* vol. 20, p. 1064–1082, 1950.

[42] F. London, H. London and F. A. Lindemann, “The electromagnetic equations of the supraconductor,” *Proceedings of the Royal Society of London. Series A - Mathematical and Physical Sciences*, vol. 149, pp. 71-88, 1935.

[43] B. D. Josephson, “Possible new effects in superconductive tunnelling,” *Physics Letters,* vol. 1, pp. 251-253, 1962.

[44] P. W. Anderson and J. M. Rowell, “Probable Observation of the Josephson Superconducting Tunneling Effect,” *Phys. Rev. Lett.,* vol. 10, no. 6, p. 230–232, March 1963.

[45] J. Bardeen, L. N. Cooper and J. R. Schrieffer, “Microscopic Theory of Superconductivity,” *Phys. Rev.,* vol. 106, no. 1, p. 162–164, April 1957.

[46] J. Bardeen, L. N. Cooper and J. R. Schrieffer, “Theory of Superconductivity,” *Phys. Rev.,* vol. 108, no. 5, p. 1175–1204, December 1957.

[47] L. P. Gor'kov, “Microscopic derivation of the Ginzburg-Landau equations in the theory of superconductivity,” *Soviet Physics JETP,* vol. 36(9), p. 1364, 1959.

[48] A. A. Abrikosov, “On the Magnetic properties of superconductors of the second group,” *Sov. Phys. JETP,* vol. 5, p. 1174–1182, 1957.

[49] A. Barone and G. Paternò, “Front Matter,” in *Physics and Applications of the Josephson Effect*, John Wiley & Sons, Ltd, 1982, pp. i-xix.

[50] K. K. Likharev, “Superconducting weak links,” *Rev. Mod. Phys.,* vol. 51, no. 1, p. 101–159, January 1979.

[51] A. D. Semenov, G. N. Goltsman and R. Sobolewski, "Hot-electron effect in superconductors and its applications for radiation sensors," *Superconductor Science and Technology,* vol. 15, p. R1–R16, March 2002.

[52] A. Rothwarf and B. N. Taylor, "Measurement of Recombination Lifetimes in Superconductors," *Phys. Rev. Lett.,* vol. 19, no. 1, p. 27–30, July 1967.

[53] A. G. Kozorezov, A. F. Volkov, J. K. Wigmore, A. Peacock, A. Poelaert and R. den Hartog, "Quasiparticle-phonon downconversion in nonequilibrium superconductors," *Phys. Rev. B,* vol. 61, no. 17, p. 11807–11819, May 2000.

[54] A. Zehnder, "Response of superconductive films to localized energy deposition," *Phys. Rev. B,* vol. 52, no. 17, p. 12858–12866, November 1995.

[55] D. Twerenbold, "Giaever-Type Superconducting Tunnelling Junctions as High-Resolution X-Ray Detectors," *Europhysics Letters (EPL),* vol. 1, p. 209–214, March 1986.

[56] A. Peacock, P. Verhoeve, N. Rando, A. van Dordrecht, B. G. Taylor, C. Erd, M. A. C. Perryman, R. Venn, J. Howlett, D. J. Goldie, J. Lumley and M. Wallis, "Single optical photon detection with a superconducting tunnel junction," *Nature,* vol. 381, p. 135–137, 1996.

[57] S. H. Moseley, J. C. Mather and D. McCammon, "Thermal detectors as x-ray spectrometers," *Journal of Applied Physics,* vol. 56, pp. 1257-1262, 1984.

[58] D. Fukuda, G. Fujii, T. Numata, K. Amemiya, A. Yoshizawa, H. Tsuchida, H. Fujino, H. Ishii, T. Itatani, S. Inoue and T. Zama, "Titanium-based transition-edge photon number resolving detector with 98% detection efficiency with index-matched small-gap fiber coupling," *Opt. Express,* vol. 19, p. 870–875, January 2011.

[59] K. D. Irwin, “SQUIDs and Transition-Edge Sensors,” *Journal of Superconductivity and Novel Magnetism,* vol. 34, p. 1601–1606, 2021.

[60] P. K. Day, H. G. LeDuc, B. A. Mazin, A. Vayonakis and J. Zmuidzinas, “A broadband superconducting detector suitable for use in large arrays,” *Nature,* vol. 425, p. 817–821, 23 October 2003.

[61] J. Gao, M. R. Vissers, M. O. Sandberg, F. C. S. da Silva, S. W. Nam, D. P. Pappas, D. S. Wisbey, E. C. Langman, S. R. Meeker, B. A. Mazin, H. G. Leduc, J. Zmuidzinas and K. D. Irwin, “A titanium-nitride near-infrared kinetic inductance photon-counting detector and its anomalous electrodynamics,” *Applied Physics Letters,* vol. 101, p. 142602, 2012.

[62] S. Rowe, E. Pascale, S. Doyle, C. Dunscombe, P. Hargrave, A. Papageorgio, K. Wood, P. A. R. Ade, P. Barry, A. Bideaud, T. Brien, C. Dodd, W. Grainger, J. House, P. Mauskopf, P. Moseley, L. Spencer, R. Sudiwala, C. Tucker and I. Walker, “A passive terahertz video camera based on lumped element kinetic inductance detectors,” *Review of Scientific Instruments,* vol. 87, p. 033105, 2016.

[63] G. N. Goltsman, O. Okunev, G. Chulkova, A. Lipatov, A. Semenov, K. Smirnov, B. Voronov, A. Dzardanov, C. Williams and R. Sobolewski, “Picosecond superconducting single-photon optical detector,” *Appl. Phys. Lett.,* vol. 79, pp. 705-707, 2001.

[64] E. A. Dauler, M. E. Grein, A. J. Kerman, F. Marsili, S. Miki, S. W. Nam, M. D. Shaw, H. Terai, V. B. Verma and T. Yamashita, “Review of superconducting nanowire single-photon detector system design options and demonstrated performance,” *Optical Engineering,* vol. 53, p. 1 – 13, 2014.

[65] A. D. Semenov, G. N. Gol'tsman and A. A. Korneev, “Quantum detection by current carrying superconducting film,” *Physica C: Superconductivity,* vol. 351, pp. 349-356, 2001.

[66] A. N. Zotova and D. Y. Vodolazov, “Photon detection by current-carrying superconducting film: A time-dependent Ginzburg-Landau approach,” *Phys. Rev. B,* vol. 85, no. 2, p. 024509, January 2012.

[67] A. Engel, J. J. Renema, K. Il'in and A. Semenov, “Detection mechanism of superconducting nanowire single-photon detectors,” *Superconductor Science and Technology,* vol. 28, p. 114003, September 2015.

[68] D. V. Reddy, R. R. Nerem, S. W. Nam, R. P. Mirin and V. B. Verma, “Superconducting nanowire single-photon detectors with 98% system detection efficiency at 1550 nm,” *Optica,* vol. 7, p. 1649–1653, December 2020.

[69] B. Korzh, Q.-Y. Zhao, J. P. Allmaras, S. Frasca, T. M. Autry, E. A. Bersin, A. D. Beyer, R. M. Briggs, B. Bumble, M. Colangelo, G. M. Crouch, A. E. Dane, T. Gerrits, A. E. Lita, F. Marsili, G. Moody, C. Peña, E. Ramirez, J. D. Rezac, N. Sinclair, M. J. Stevens, A. E. Velasco, V. B. Verma, E. E. Wollman, S. Xie, D. Zhu, P. D. Hale, M. Spiropulu, K. L. Silverman, R. P. Mirin, S. W. Nam, A. G. Kozorezov, M. D. Shaw and K. K. Berggren, “Demonstration of sub-3 ps temporal resolution with a superconducting nanowire single-photon detector,” *Nature Photonics,* vol. 14, p. 250–255, 2020.

[70] A. E. Lita, A. J. Miller and S. W. Nam, “Counting near-infrared single-photons with 95% efficiency,” *Opt. Express,* vol. 16, p. 3032–3040, March 2008.

[71] A. Shurakov, Y. Lobanov and G. Goltsman, “Superconducting hot-electron bolometer: from the discovery of hot-electron phenomena to practical

applications," *Superconductor Science and Technology,* vol. 29, p. 023001, December 2015.

[72] B. S. Karasik, A. V. Sergeev and D. E. Prober, "Nanobolometers for THz Photon Detection," *Terahertz Science and Technology, IEEE Transactions on,* vol. 1, pp. 97-111, September 2011.

[73] S. Friedrich, "Superconducting Tunnel Junction Photon Detectors: Theory and Applications," *Journal of Low Temperature Physics,* vol. 151, p. 277–286, 2008.

[74] A. E. Lita, B. Calkins, L. A. Pellouchoud, A. J. Miller and S. Nam, "Superconducting transition-edge sensors optimized for high-efficiency photon-number resolving detectors," *Proc. SPIE,* vol. 7681, p. 71 – 80, 2010.

[75] S. Doyle, P. Mauskopf, J. Naylon, A. Porch and C. Duncombe, "Lumped Element Kinetic Inductance Detectors," *Journal of Low Temperature Physics,* vol. 151, p. 530–536, 2008.

[76] L. You, "Superconducting nanowire single-photon detectors for quantum information," *Nanophotonics,* vol. 9, p. 2673–2692, 2020.

[77] J. Wei, D. Olaya, B. S. Karasik, S. V. Pereverzev, A. V. Sergeev and M. E. Gershenson, "Ultrasensitive hot-electron nanobolometers for terahertz astrophysics," *Nature Nanotechnology,* vol. 3, p. 496–500, 2008.

[78] A. J. Kreisler and A. Gaugue, "Recent progress in high-temperature superconductor bolometric detectors: from the mid-infrared to the far-infrared (THz) range," *Superconductor Science and Technology,* vol. 13, p. 1235–1245, July 2000.

[79] C. Yang, R. R. Niu, Z. S. Guo, X. W. Cai, H. M. Chu, K. Yang, Y. Wang, Q. R. Feng and Z. Z. Gan, "Lumped element kinetic inductance detectors based on two-gap MgB2 thin films," *Applied Physics Letters,* vol. 112, p. 022601, 2018.

[80] S. Cherednichenko, N. Acharya, E. Novoselov and V. Drakinskiy, "Low kinetic inductance superconducting MgB2 nanowires with a 130 ps relaxation time for single-photon detection applications," *Superconductor Science and Technology,* vol. 34, p. 044001, February 2021.

[81] M. A. Lindeman, J. A. Bonetti, B. Bumble, P. K. Day, B. H. Eom, W. A. Holmes and A. W. Kleinsasser, "Arrays of membrane isolated yttrium-barium-copper-oxide kinetic inductance bolometers," *Journal of Applied Physics,* vol. 115, p. 234509, 2014.

[82] R. Arpaia, M. Ejrnaes, L. Parlato, F. Tafuri, R. Cristiano, D. Golubev, R. Sobolewski, T. Bauch, F. Lombardi and G. P. Pepe, "High-temperature superconducting nanowires for photon detection," *Physica C: Superconductivity and its Applications,* vol. 509, pp. 16-21, 2015.

[83] B. A. Mazin, "Superconducting Materials for Microwave Kinetic Inductance Detectors," *arXiv:2004.14576*, 2020.

[84] A. Banerjee, L. J. Baker, A. Doye, M. Nord, R. M. Heath, K. Erotokritou, D. Bosworth, Z. H. Barber, I. MacLaren and R. H. Hadfield, "Characterisation of amorphous molybdenum silicide (MoSi) superconducting thin films and nanowires," *Superconductor Science and Technology,* vol. 30, p. 084010, July 2017.

[85] V. B. Verma, A. E. Lita, M. R. Vissers, F. Marsili, D. P. Pappas, R. P. Mirin and S. W. Nam, "Superconducting nanowire single photon detectors fabricated from

an amorphous Mo0.75Ge0.25 thin film,” *Applied Physics Letters,* vol. 105, p. 022602, 2014.

[86] V. Ganni and J. Fesmire, “Cryogenics for superconductors: Refrigeration, delivery, and preservation of the cold,” *AIP Conference Proceedings,* vol. 1434, pp. 15-27, 2012.

[87] R. Radenbaugh, “Refrigeration for superconductors,” *Proceedings of the IEEE,* vol. 92, pp. 1719-1734, 2004.

[88] R. H. Hadfield, M. J. Stevens, S. S. Gruber, A. J. Miller, R. E. Schwall, R. P. Mirin and S. W. Nam, “Single photon source characterization with a superconducting single photon detector,” *Opt. Express,* vol. 13, p. 10846–10853, December 2005.

[89] N. R. Gemmell, M. Hills, T. Bradshaw, T. Rawlings, B. Green, R. M. Heath, K. Tsimvrakidis, S. Dobrovolskiy, V. Zwiller, S. N. Dorenbos, M. Crook and R. H. Hadfield, “A miniaturized 4 K platform for superconducting infrared photon counting detectors,” *Superconductor Science and Technology,* vol. 30, p. 11LT01, September 2017.

[90] X. Xi, J. Wang, L. Chen, Y. Zhou and J. Wang, “Progress and Challenges of Sub-Kelvin Sorption Cooler and Its Prospects for Space Application,” *Journal of Low Temperature Physics,* vol. 199, p. 1363–1381, 2020.

[91] S. Oguri, H. Ishitsuka, J. Choi, M. Kawai and O. Tajima, “Note: Sub-Kelvin refrigeration with dry-coolers on a rotating system,” *Review of Scientific Instruments,* vol. 85, p. 086101, 2014.

[92] G. M. Klemencic, P. A. R. Ade, S. Chase, R. Sudiwala and A. L. Woodcraft, “A continuous dry 300 mK cooler for THz sensing applications,” *Review of Scientific Instruments,* vol. 87, p. 045107, 2016.

[93] M. J. Devlin, S. R. Dicker, J. Klein and M. P. Supanich, “A high capacity completely closed-cycle 250 mK 3He refrigeration system based on a pulse tube cooler,” *Cryogenics,* vol. 44, pp. 611-616, 2004.

[94] A. M. Clark, N. A. Miller, A. Williams, S. T. Ruggiero, G. C. Hilton, L. R. Vale, J. A. Beall, K. D. Irwin and J. N. Ullom, “Cooling of bulk material by electron-tunneling refrigerators,” *Applied Physics Letters,* vol. 86, p. 173508, 2005.

[95] A. T. A. M. de Waele, “Basic Operation of Cryocoolers and Related Thermal Machines,” *Journal of Low Temperature Physics,* vol. 164, p. 179, 2011.

[96] G. Teleberg, S. T. Chase and L. Piccirillo, “A Cryogen-Free Miniature Dilution Refrigerator for Low-Temperature Detector Applications,” *Journal of Low Temperature Physics,* vol. 151, p. 669–674, 2008.

[97] M. Balli, S. Jandl, P. Fournier and A. Kedous-Lebouc, “Advanced materials for magnetic cooling: Fundamentals and practical aspects,” *Applied Physics Reviews,* vol. 4, p. 021305, 2017.

[98] P. P. P. M. Lerou, G. C. F. Venhorst, C. F. Berends, T. T. Veenstra, M. Blom, J. F. Burger, H. J. M. ter Brake and H. Rogalla, “Fabrication of a micro cryogenic cold stage using MEMS-technology,” vol. 16, p. 1919–1925, August 2006.

[99] H. S. Cao and H. J. M. ter Brake, “Progress in and Outlook for Cryogenic Microcooling,” *Phys. Rev. Applied,* vol. 14, no. 4, p. 044044, October 2020.

[100] M. M. Leivo, J. P. Pekola and D. V. Averin, “Efficient Peltier refrigeration by a pair of normal metal/insulator/superconductor junctions,” *Applied Physics Letters,* vol. 68, pp. 1996-1998, 1996.

[101] J. Dreyling-Eschweiler, N. Bastidon, B. Döbrich, D. Horns, F. Januschek and A. Lindner, “Characterization, 1064 nm photon signals and background events of a tungsten TES detector for the ALPS experiment,” *Journal of Modern Optics,* vol. 62, pp. 1132-1140, 2015.

[102] R. Bähre, B. Döbrich, J. Dreyling-Eschweiler, S. Ghazaryan, R. Hodajerdi, D. Horns, F. Januschek, E. A. Knabbe, A. Lindner, D. Notz, A. Ringwald, J. E. von Seggern, R. Stromhagen, D. Trines and B. Willke, “Any light particle search II — Technical Design Report,” vol. 8, p. T09001–T09001, September 2013.

[103] M. Kurakado, “Possibility of high resolution detectors using superconducting tunnel junctions,” *Nuclear Instruments and Methods in Physics Research,* vol. 196, pp. 275-277, 1982.

[104] N. Rando, A. Peacock, A. van Dordrecht, C. Foden, R. Engelhardt, B. G. Taylor, P. Gare, J. Lumley and C. Pereira, “The properties of niobium superconducting tunneling junctions as X-ray detectors,” *Nuclear Instruments and Methods in Physics Research Section A: Accelerators, Spectrometers, Detectors and Associated Equipment,* vol. 313, pp. 173-195, 1992.

[105] D. D. E. Martin, P. Verhoeve, T. Oosterbroek, R. Hijmering, A. Peacock and R. Schulz, “Accurate time-resolved optical photospectroscopy with superconducting tunnel junction arrays,” *Proc. SPIE,* vol. 6269, p. 238 – 248, 2006.

[106] M. Nahum and J. M. Martinis, “Ultrasensitive-hot-electron microbolometer,” *Appl. Phys. Lett.,* vol. 63, pp. 3075-3077, 1993.

[107] M. Nahum, T. M. Eiles and J. M. Martinis, “Electronic microrefrigerator based on a normal-insulator-superconductor tunnel junction,” *Appl. Phys. Lett.,* vol. 65, pp. 3123-3125, 1994.

[108] L. S. Kuzmin, A. L. Pankratov, A. V. Gordeeva, V. O. Zbrozhek, V. A. Shamporov, L. S. Revin, A. V. Blagodatkin, S. Masi and P. de Bernardis, “Photon-noise-limited cold-electron bolometer based on strong electron self-cooling for high-performance cosmology missions,” *Communications Physics,* vol. 2, p. 104, 2019.

[109] T. L. R. Brien, P. A. R. Ade, P. S. Barry, C. Dunscombe, D. R. Leadley, D. V. Morozov, M. Myronov, E. H. C. Parker, M. J. Prest, M. Prunnila, R. V. Sudiwala, T. E. Whall and P. D. Mauskopf, “A strained silicon cold electron bolometer using Schottky contacts,” *Applied Physics Letters,* vol. 105, p. 043509, 2014.

[110] D. Morozov, I. Bacchus, P. Mauskopf, M. Elliott, C. Dunscombe, M. Henini and M. Hopkinson, “High-sensitivity terahertz detector using two-dimensional electron gas absorber and tunnel junction contacts as a thermometer,” *Proc. SPIE,* vol. 6275, p. 559 – 567, 2006.

[111] S. Friedrich, T. Funk, O. Drury, S. E. Labov and S. P. Cramer, “A multichannel superconducting soft x-ray spectrometer for high-resolution spectroscopy of dilute samples,” *Review of Scientific Instruments,* vol. 73, pp. 1629-1631, 2002.

[112] S. Friedrich, O. B. Drury, S. P. Cramer and P. G. Green, “A 36-pixel superconducting tunnel junction soft X-ray detector for environmental science

applications," *Nuclear Instruments and Methods in Physics Research Section A: Accelerators, Spectrometers, Detectors and Associated Equipment,* vol. 559, pp. 776-778, 2006.

[113] S. Friedrich, "Cryogenic X-ray detectors for synchrotron science," *Journal of Synchrotron Radiation,* vol. 13, p. 159–171, March 2006.

[114] T. T. Heikkilä, R. Ojajärvi, I. J. Maasilta, E. Strambini, F. Giazotto and F. S. Bergeret, "Thermoelectric Radiation Detector Based on Superconductor-Ferromagnet Systems," *Phys. Rev. Applied,* vol. 10, no. 3, p. 034053, September 2018.

[115] Z. Geng, A. P. Helenius, T. T. Heikkilä and I. J. Maasilta, "Superconductor-Ferromagnet Tunnel Junction Thermoelectric Bolometer and Calorimeter with a SQUID Readout," *Journal of Low Temperature Physics,* vol. 199, p. 585–592, 2020.

[116] F. Vischi, M. Carrega, A. Braggio, F. Paolucci, F. Bianco, S. Roddaro and F. Giazotto, "Electron Cooling with Graphene-Insulator-Superconductor Tunnel Junctions for Applications in Fast Bolometry," *Phys. Rev. Applied,* vol. 13, no. 5, p. 054006, May 2020.

[117] E. D. Walsh, W. Jung, G.-H. Lee, D. K. Efetov, B.-I. Wu, K.-F. Huang, O. A. Thomas, T. Taniguchi, K. Watanabe, P. Kim, D. Englund and K. C. Fong, "Josephson junction infrared single-photon detector," *Science,* vol. 372, p. 409–412, April 2021.

[118] K. D. Irwin and G. C. Hilton, "Transition-Edge Sensors," in *Cryogenic Particle Detection,* C. Enss, Ed., Berlin, Heidelberg: Springer Berlin Heidelberg, 2005, p. 63–150.

[119] P. A. J. de Korte, H. F. C. Hoevers, J.-W. den Herder, J. A. M. Bleeker, W. B. Tiest, M. P. Bruijn, M. L. Ridder, R. J. Wiegerink, J. S. Kaastra, J. van der Kuur and W. A. Mels, “TES x-ray calorimeter-array for imaging spectroscopy,” *Proc. SPIE,* vol. 4851, p. 779 – 789, 2003.

[120] D. Morozov, P. D. Mauskopf, P. Ade, M. Ridder, P. Khosropanah, M. Bruijn, J. van der Kuur, H. Hoevers, J. R. Gao and D. Griffin, “Ultrasensitive TES bolometers for space based FIR astronomy,” *IEEE Trans. Appl. Supercond.,* vol. 21, pp. 188-191, June 2011.

[121] T. Gerrits, B. Calkins, N. Tomlin, A. E. Lita, A. Migdall, R. Mirin and S. W. Nam, “Extending single-photon optimized superconducting transition edge sensors beyond the single-photon counting regime,” *Opt. Express,* vol. 20, p. 23798–23810, October 2012.

[122] G. Di Giuseppe, M. Atatüre, M. D. Shaw, A. V. Sergienko, B. E. A. Saleh, M. C. Teich, A. J. Miller, S. W. Nam and J. Martinis, “Direct observation of photon pairs at a single output port of a beam-splitter interferometer,” *Phys. Rev. A,* vol. 68, no. 6, p. 063817, December 2003.

[123] B. G. Christensen, K. T. McCusker, J. B. Altepeter, B. Calkins, T. Gerrits, A. E. Lita, A. Miller, L. K. Shalm, Y. Zhang, S. W. Nam, N. Brunner, C. C. W. Lim, N. Gisin and P. G. Kwiat, “Detection-Loophole-Free Test of Quantum Nonlocality, and Applications,” *Phys. Rev. Lett.,* vol. 111, no. 13, p. 130406, September 2013.

[124] M. Giustina, M. A. M. Versteegh, S. Wengerowsky, J. Handsteiner, A. Hochrainer, K. Phelan, F. Steinlechner, J. Kofler, J.-Å. Larsson, C. Abellán, W. Amaya, V. Pruneri, M. W. Mitchell, J. Beyer, T. Gerrits, A. E. Lita, L. K. Shalm,

S. W. Nam, T. Scheidl, R. Ursin, B. Wittmann and A. Zeilinger, “Significant-Loophole-Free Test of Bell's Theorem with Entangled Photons,” *Phys. Rev. Lett.*, vol. 115, no. 25, p. 250401, December 2015.

[125] Z. H. Levine, B. L. Glebov, A. L. Pintar and A. L. Migdall, “Absolute calibration of a variable attenuator using few-photon pulses,” *Opt. Express*, vol. 23, p. 16372–16382, June 2015.

[126] J. M. Arrazola, V. Bergholm, K. Brádler, T. R. Bromley, M. J. Collins, I. Dhand, A. Fumagalli, T. Gerrits, A. Goussev, L. G. Helt, J. Hundal, T. Isacsson, R. B. Israel, J. Izaac, S. Jahangiri, R. Janik, N. Killoran, S. P. Kumar, J. Lavoie, A. E. Lita, D. H. Mahler, M. Menotti, B. Morrison, S. W. Nam, L. Neuhaus, H. Y. Qi, N. Quesada, A. Repingon, K. K. Sabapathy, M. Schuld, D. Su, J. Swinarton, A. Száva, K. Tan, P. Tan, V. D. Vaidya, Z. Vernon, Z. Zabaneh and Y. Zhang, “Quantum circuits with many photons on a programmable nanophotonic chip,” *Nature*, vol. 591, p. 54–60, 2021.

[127] M. D. Audley, W. S. Holland, W. D. Duncan, D. Atkinson, M. Cliffe, M. Ellis, X. Gao, D. C. Gostick, T. Hodson, D. Kelly, M. J. MacIntosh, H. McGregor, T. Peacocke, I. Robson, I. Smith, K. D. Irwin, G. C. Hilton, J. N. Ullom, A. Walton, C. Dunare, W. Parkes, P. A. R. Ade, D. Bintley, F. Gannaway, M. Griffin, G. Pisano, R. V. Sudiwala, I. Walker, A. Woodcraft, M. Fich, M. Halpern, G. Mitchell, D. Naylor and P. Bastien, “SCUBA-2: A large-format TES array for submillimetre astronomy,” *Nuclear Instruments and Methods in Physics Research Section A: Accelerators, Spectrometers, Detectors and Associated Equipment*, vol. 520, pp. 479-482, 2004.

[128] R. den Hartog, M. D. Audley, J. Beyer, D. Boersma, M. Bruijn, L. Gottardi, H. Hoevers, R. Hou, G. Keizer, P. Khosropanah, M. Kiviranta, P. de Korte, J. van der Kuur, B.-J. van Leeuwen, A. C. T. Nieuwenhuizen and P. van Winden, "Low-Noise Readout of TES Detectors with Baseband Feedback Frequency Domain Multiplexing," *Journal of Low Temperature Physics*, vol. 167, p. 652–657, 2012.

[129] A. G. Kozorezov, C. Lambert, F. Marsili, M. J. Stevens, V. B. Verma, J. A. Stern, R. Horansky, S. Dyer, S. Duff, D. P. Pappas, A. Lita, M. D. Shaw, R. P. Mirin and S. W. Nam, "Quasiparticle recombination in hotspots in superconducting current-carrying nanowires," *Phys. Rev. B,* vol. 92, no. 6, p. 064504, August 2015.

[130] D. Y. Vodolazov, Y. P. Korneeva, A. V. Semenov, A. A. Korneev and G. N. Goltsman, "Vortex-assisted mechanism of photon counting in a superconducting nanowire single-photon detector revealed by external magnetic field," *Phys. Rev. B,* vol. 92, no. 10, p. 104503, September 2015.

[131] A. D. Semenov, "Superconducting nanostrip single-photon detectors some fundamental aspects in detection mechanism, technology and performance," *Superconductor Science and Technology*, vol. 34, p. 054002, April 2021.

[132] M. G. Tanner, C. M. Natarajan, V. K. Pottapenjara, J. A. O'Connor, R. J. Warburton, R. H. Hadfield, B. Baek, S. Nam, S. N. Dorenbos, E. B. Ureña, T. Zijlstra, T. M. Klapwijk and V. Zwiller, "Enhanced telecom wavelength single-photon detection with NbTiN superconducting nanowires on oxidized silicon," *Applied Physics Letters*, vol. 96, p. 221109, 2010.

[133] K. S. Il'in, M. Lindgren, M. Currie, A. D. Semenov, G. N. Gol'tsman, R. Sobolewski, S. I. Cherednichenko and E. M. Gershenzon, “Picosecond hot-electron energy relaxation in NbN superconducting photodetectors,” *Applied Physics Letters*, vol. 76, pp. 2752-2754, 2000.

[134] A. Engel, A. Aeschbacher, K. Inderbitzin, A. Schilling, K. Il’in, M. Hofherr, M. Siegel, A. Semenov and H.-W. Hübers, “Tantalum nitride superconducting single-photon detectors with low cut-off energy,” *Applied Physics Letters,* vol. 100, p. 062601, 2012.

[135] Y. Korneeva, I. Florya, S. Vdovichev, M. Moshkova, N. Simonov, N. Kaurova, A. Korneev and G. Goltsman, “Comparison of Hot Spot Formation in NbN and MoN Thin Superconducting Films After Photon Absorption,” *IEEE Transactions on Applied Superconductivity,* vol. 27, pp. 1-4, 2017.

[136] A. J. Annunziata, O. Quaranta, D. F. Santavicca, A. Casaburi, L. Frunzio, M. Ejrnaes, M. J. Rooks, R. Cristiano, S. Pagano, A. Frydman and D. E. Prober, “Reset dynamics and latching in niobium superconducting nanowire single-photon detectors,” *Journal of Applied Physics,* vol. 108, p. 084507, 2010.

[137] B. Baek, A. E. Lita, V. Verma and S. W. Nam, “Superconducting a-WxSi1−x nanowire single-photon detector with saturated internal quantum efficiency from visible to 1850 nm,” *Applied Physics Letters,* vol. 98, p. 251105, 2011.

[138] Y. P. Korneeva, M. Y. Mikhailov, Y. P. Pershin, N. N. Manova, A. V. Divochiy, Y. B. Vakhtomin, A. A. Korneev, K. V. Smirnov, A. G. Sivakov, A. Y. Devizenko and G. N. Goltsman, “Superconducting single-photon detector made of MoSi film,” *Superconductor Science and Technology,* vol. 27, p. 095012, August 2014.

[139] F. Marsili, B. Verma V., A. Stern J., S. Harrington, E. Lita A., T. Gerrits, I. Vayshenker, B. Baek, D. Shaw M., P. Mirin R. and W. Nam S., “Detecting single infrared photons with 93% system efficiency,” *Nat Photon,* vol. 7, p. 210–214, March 2013.

[140] G. G. Taylor, D. V. Morozov, C. T. Lennon, P. S. Barry, C. Sheagren and R. H. Hadfield, “Infrared single-photon sensitivity in atomic layer deposited superconducting nanowires,” *Applied Physics Letters,* vol. 118, p. 191106, 2021.

[141] H. Shibata, T. Akazaki and Y. Tokura, “Fabrication of MgB2Nanowire Single-Photon Detector with Meander Structure,” *Applied Physics Express,* vol. 6, p. 023101, February 2013.

[142] M. Ejrnaes, L. Parlato, R. Arpaia, T. Bauch, F. Lombardi, R. Cristiano, F. Tafuri and G. P. Pepe, “Observation of dark pulses in 10 nm thick YBCO nanostrips presenting hysteretic current voltage characteristics,” *Superconductor Science and Technology,* vol. 30, p. 12LT02, November 2017.

[143] P. Seifert, J. R. D. Retamal, R. L. Merino, H. H. Sheinfux, J. N. Moore, M. A. Aamir, T. Taniguchi, K. Watanabe, K. Kadowaki, M. Artiglia, M. Romagnoli and D. K. Efetov, “A high-T c van der Waals superconductor based photodetector with ultra-high responsivity and nanosecond relaxation time,” *2D Materials,* vol. 8, p. 035053, June 2021.

[144] G. J. Orchin, D. De Fazio, A. Di Bernardo, M. Hamer, D. Yoon, A. R. Cadore, I. Goykhman, K. Watanabe, T. Taniguchi, J. W. A. Robinson, R. V. Gorbachev, A. C. Ferrari and R. H. Hadfield, “Niobium diselenide superconducting photodetectors,” *Applied Physics Letters,* vol. 114, p. 251103, 2019.

[145] A. Verevkin, J. Zhang, R. Sobolewski, A. Lipatov, O. Okunev, G. Chulkova, A. Korneev, K. Smirnov, G. N. Gol'tsman and A. Semenov, “Detection efficiency of large-active-area NbN single-photon superconducting detectors in the ultraviolet to near-infrared range,” *Appl. Phys. Lett.*, vol. 80, pp. 4687-4689, 2002.

[146] K. M. Rosfjord, J. K. W. Yang, E. A. Dauler, A. J. Kerman, V. Anant, B. M. Voronov, G. N. Gol'tsman and K. K. Berggren, “Nanowire Single-photon detector with an integrated optical cavity and anti-reflection coating,” *Opt. Express*, vol. 14, p. 527–534, January 2006.

[147] S. Miki, T. Yamashita, H. Terai and Z. Wang, “High performance fiber-coupled NbTiN superconducting nanowire single photon detectors with Gifford-McMahon cryocooler,” *Opt. Express*, vol. 21, p. 10208–10214, April 2013.

[148] I. E. Zadeh, J. W. N. Los, R. B. M. Gourgues, V. Steinmetz, G. Bulgarini, S. M. Dobrovolskiy, V. Zwiller and S. N. Dorenbos, “Single-photon detectors combining high efficiency, high detection rates, and ultra-high timing resolution,” *APL Photonics*, vol. 2, p. 111301, 2017.

[149] W. Zhang, L. You, H. Li, J. Huang, C. Lv, L. Zhang, X. Liu, J. Wu, Z. Wang and X. Xie, “NbN superconducting nanowire single photon detector with efficiency over 90% at 1550 nm wavelength operational at compact cryocooler temperature,” *Science China Physics, Mechanics & Astronomy*, vol. 60, p. 120314, 2017.

[150] K. Erotokritou, R. M. Heath, G. G. Taylor, C. Tian, A. Banerjee, A. Casaburi, C. M. Natarajan, S. Miki, H. Terai and R. H. Hadfield, “Nano-optical photoresponse mapping of superconducting nanowires with enhanced near

infrared absorption," *Superconductor Science and Technology,* vol. 31, p. 125012, November 2018.

[151] R. M. Heath, M. G. Tanner, T. D. Drysdale, S. Miki, V. Giannini, S. A. Maier and R. H. Hadfield, "Nanoantenna Enhancement for Telecom-Wavelength Superconducting Single Photon Detectors," *Nano Lett.,* vol. 15, p. 819–822, February 2015.

[152] X. Hu, E. A. Dauler, R. J. Molnar and K. K. Berggren, "Superconducting nanowire single-photon detectors integrated with optical nano-antennae," *Opt. Express,* vol. 19, p. 17–31, January 2011.

[153] J. P. Sprengers, A. Gaggero, D. Sahin, S. Jahanmirinejad, G. Frucci, F. Mattioli, R. Leoni, J. Beetz, M. Lermer, M. Kamp, S. Höfling, R. Sanjines and A. Fiore, "Waveguide superconducting single-photon detectors for integrated quantum photonic circuits," *Applied Physics Letters,* vol. 99, p. 181110, 2011.

[154] W. H. P. Pernice, C. Schuck, O. Minaeva, M. Li, G. N. Goltsman, A. V. Sergienko and H. X. Tang, "High-speed and high-efficiency travelling wave single-photon detectors embedded in nanophotonic circuits," *Nature Communications,* vol. 3, p. 1325, 2012.

[155] F. Najafi, J. Mower, N. C. Harris, F. Bellei, A. Dane, C. Lee, X. Hu, P. Kharel, F. Marsili, S. Assefa, K. K. Berggren and D. Englund, "On-chip detection of non-classical light by scalable integration of single-photon detectors," *Nature Communications,* vol. 6, p. 5873, 2015.

[156] M. K. Akhlaghi, E. Schelew and J. F. Young, "Waveguide integrated superconducting single-photon detectors implemented as near-perfect absorbers of coherent radiation," *Nature Communications,* vol. 6, p. 8233, 2015.

[157] J. Li, R. A. Kirkwood, L. J. Baker, D. Bosworth, K. Erotokritou, A. Banerjee, R. M. Heath, C. M. Natarajan, Z. H. Barber, M. Sorel and R. H. Hadfield, "Nano-optical single-photon response mapping of waveguide integrated molybdenum silicide (MoSi) superconducting nanowires," *Opt. Express,* vol. 24, p. 13931–13938, June 2016.

[158] R. H. Hadfield, "Superfast photon counting," *Nature Photonics,* vol. 14, p. 201–202, 2020.

[159] A. N. McCaughan, "Readout architectures for superconducting nanowire single photon detectors," *Superconductor Science and Technology,* vol. 31, p. 040501, February 2018.

[160] M. S. Allman, V. B. Verma, M. Stevens, T. Gerrits, R. D. Horansky, A. E. Lita, F. Marsili, A. Beyer, M. D. Shaw, D. Kumor, R. Mirin and S. W. Nam, "A near-infrared 64-pixel superconducting nanowire single photon detector array with integrated multiplexed readout," *Applied Physics Letters,* vol. 106, p. 192601, 2015.

[161] J. P. Allmaras, E. E. Wollman, A. D. Beyer, R. M. Briggs, B. A. Korzh, B. Bumble and M. D. Shaw, "Demonstration of a Thermally Coupled Row-Column SNSPD Imaging Array," *Nano Lett.,* vol. 20, p. 2163–2168, March 2020.

[162] H. Terai, S. Miki, T. Yamashita, K. Makise and Z. Wang, "Demonstration of single-flux-quantum readout operation for superconducting single-photon detectors," *Applied Physics Letters,* vol. 97, p. 112510, 2010.

[163] T. Ortlepp, M. Hofherr, L. Fritzsch, S. Engert, K. Ilin, D. Rall, H. Toepfer, H.-G. Meyer and M. Siegel, "Demonstration of digital readout circuit for

superconducting nanowire single photon detector," *Opt. Express,* vol. 19, p. 18593–18601, September 2011.

[164] M. Yabuno, S. Miyajima, S. Miki and H. Terai, "Scalable implementation of a superconducting nanowire single-photon detector array with a superconducting digital signal processor," *Opt. Express,* vol. 28, p. 12047–12057, April 2020.

[165] S. Doerner, A. Kuzmin, S. Wuensch, I. Charaev, F. Boes, T. Zwick and M. Siegel, "Frequency-multiplexed bias and readout of a 16-pixel superconducting nanowire single-photon detector array," *Applied Physics Letters,* vol. 111, p. 032603, 2017.

[166] M. de Cea, E. E. Wollman, A. H. Atabaki, D. J. Gray, M. D. Shaw and R. J. Ram, "Photonic Readout of Superconducting Nanowire Single Photon Counting Detectors," *Scientific Reports,* vol. 10, p. 9470, 2020.

[167] E. E. Wollman, V. B. Verma, A. E. Lita, W. H. Farr, M. D. Shaw, R. P. Mirin and S. W. Nam, "Kilopixel array of superconducting nanowire single-photon detectors," *Opt. Express,* vol. 27, p. 35279–35289, November 2019.

[168] R. H. Hadfield, J. L. Habif, J. Schlafer, R. E. Schwall and S. W. Nam, "Quantum key distribution at 1550nm with twin superconducting single-photon detectors," *Applied Physics Letters,* vol. 89, p. 241129, 2006.

[169] H. Takesue, S. W. Nam, Q. Zhang, R. H. Hadfield, T. Honjo, K. Tamaki and Y. Yamamoto, "Quantum key distribution over a 40-dB channel loss using superconducting single-photon detectors," *Nature Photonics,* vol. 1, p. 343–348, 2007.

[170] Y.-L. Tang, H.-L. Yin, S.-J. Chen, Y. Liu, W.-J. Zhang, X. Jiang, L. Zhang, J. Wang, L.-X. You, J.-Y. Guan, D.-X. Yang, Z. Wang, H. Liang, Z. Zhang, N.

Zhou, X. Ma, T.-Y. Chen, Q. Zhang and J.-W. Pan, “Measurement-Device-Independent Quantum Key Distribution over 200 km,” *Phys. Rev. Lett.,* vol. 113, no. 19, p. 190501, November 2014.

[171] P. Sibson, C. Erven, M. Godfrey, S. Miki, T. Yamashita, M. Fujiwara, M. Sasaki, H. Terai, M. G. Tanner, C. M. Natarajan, R. H. Hadfield, J. L. O’Brien and M. G. Thompson, “Chip-based quantum key distribution,” *Nature Communications,* vol. 8, p. 13984, 2017.

[172] A. Boaron, G. Boso, D. Rusca, C. Vulliez, C. Autebert, M. Caloz, M. Perrenoud, G. Gras, F. Bussières, M.-J. Li, D. Nolan, A. Martin and H. Zbinden, “Secure Quantum Key Distribution over 421 km of Optical Fiber,” *Phys. Rev. Lett.,* vol. 121, no. 19, p. 190502, November 2018.

[173] S. Wengerowsky, S. K. Joshi, F. Steinlechner, J. R. Zichi, S. M. Dobrovolskiy, R. van der Molen, J. W. N. Los, V. Zwiller, M. A. M. Versteegh, A. Mura, D. Calonico, M. Inguscio, H. Hübel, L. Bo, T. Scheidl, A. Zeilinger, A. Xuereb and R. Ursin, “Entanglement distribution over a 96-km-long submarine optical fiber,” *Proceedings of the National Academy of Sciences,* vol. 116, p. 6684–6688, 2019.

[174] H. Liu, C. Jiang, H.-T. Zhu, M. Zou, Z.-W. Yu, X.-L. Hu, H. Xu, S. Ma, Z. Han, J.-P. Chen, Y. Dai, S.-B. Tang, W. Zhang, H. Li, L. You, Z. Wang, Y. Hua, H. Hu, H. Zhang, F. Zhou, Q. Zhang, X.-B. Wang, T.-Y. Chen and J.-W. Pan, “Field Test of Twin-Field Quantum Key Distribution through Sending-or-Not-Sending over 428 km,” *Phys. Rev. Lett.,* vol. 126, no. 25, p. 250502, June 2021.

[175] K. De Greve, L. Yu, P. L. McMahon, J. S. Pelc, C. M. Natarajan, N. Y. Kim, E. Abe, S. Maier, C. Schneider, M. Kamp, S. Höfling, R. H. Hadfield, A. Forchel,

M. M. Fejer and Y. Yamamoto, “Quantum-dot spin-photon entanglement via frequency downconversion to telecom wavelength,” *Nature,* vol. 491, p. 421–425, 2012.

[176] K. De Greve, P. L. McMahon, L. Yu, J. S. Pelc, C. Jones, C. M. Natarajan, N. Y. Kim, E. Abe, S. Maier, C. Schneider, M. Kamp, S. Höfling, R. H. Hadfield, A. Forchel, M. M. Fejer and Y. Yamamoto, “Complete tomography of a high-fidelity solid-state entangled spin-photon qubit pair,” *Nature Communications,* vol. 4, p. 2228, 2013.

[177] L. Yu, C. M. Natarajan, T. Horikiri, C. Langrock, J. S. Pelc, M. G. Tanner, E. Abe, S. Maier, C. Schneider, S. Höfling, M. Kamp, R. H. Hadfield, M. M. Fejer and Y. Yamamoto, “Two-photon interference at telecom wavelengths for time-bin-encoded single photons from quantum-dot spin qubits,” *Nature Communications,* vol. 6, p. 8955, 2015.

[178] D. Lago-Rivera, S. Grandi, J. V. Rakonjac, A. Seri and H. de Riedmatten, “Telecom-heralded entanglement between multimode solid-state quantum memories,” *Nature,* vol. 594, p. 37–40, 2021.

[179] D. M. Boroson, B. S. Robinson, D. V. Murphy, D. A. Burianek, F. Khatri, J. M. Kovalik, Z. Sodnik and D. M. Cornwell, “Overview and results of the Lunar Laser Communication Demonstration,” *Proc. SPIE,* vol. 8971, p. 213 – 223, 2014.

[180] A. Biswas, M. Srinivasan, S. Piazzolla and D. Hoppe, “Deep space optical communications,” *Proc. SPIE,* vol. 10524, p. 242 – 252, 2018.

[181] D. G. Messerschmitt, P. Lubin and I. Morrison, “Challenges in Scientific Data Communication from Low-mass Interstellar Probes,” *The Astrophysical Journal Supplement Series,* vol. 249, p. 36, August 2020.

[182] J. L. O'Brien, A. Furusawa and J. Vučković, “Photonic quantum technologies,” *Nature Photonics,* vol. 3, p. 687–695, 2009.

[183] J. Wang, F. Sciarrino, A. Laing and M. G. Thompson, “Integrated photonic quantum technologies,” *Nature Photonics,* vol. 14, p. 273–284, 2020.

[184] H.-S. Zhong, Y.-H. Deng, J. Qin, H. Wang, M.-C. Chen, L.-C. Peng, Y.-H. Luo, D. Wu, S.-Q. Gong, H. Su, Y. Hu, P. Hu, X.-Y. Yang, W.-J. Zhang, H. Li, Y. Li, X. Jiang, L. Gan, G. Yang, L. You, Z. Wang, L. Li, N.-L. Liu, J. J. Renema, C.-Y. Lu and J.-W. Pan, “Phase-Programmable Gaussian Boson Sampling Using Stimulated Squeezed Light,” *Phys. Rev. Lett.,* vol. 127, no. 18, p. 180502, October 2021.

[185] J. M. Shainline, S. M. Buckley, R. P. Mirin and S. W. Nam, “Superconducting Optoelectronic Circuits for Neuromorphic Computing,” *Phys. Rev. Applied,* vol. 7, no. 3, p. 034013, March 2017.

[186] N. R. Gemmell, A. McCarthy, B. Liu, M. G. Tanner, S. D. Dorenbos, V. Zwiller, M. S. Patterson, G. S. Buller, B. C. Wilson and R. H. Hadfield, “Singlet oxygen luminescence detection with a fiber-coupled superconducting nanowire single-photon detector,” *Opt. Express,* vol. 21, p. 5005–5013, February 2013.

[187] Y. Hochberg, I. Charaev, S.-W. Nam, V. Verma, M. Colangelo and K. K. Berggren, “Detecting Sub-GeV Dark Matter with Superconducting Nanowires,” *Phys. Rev. Lett.,* vol. 123, no. 15, p. 151802, October 2019.

[188] J. Chiles, I. Charaev, R. Lasenby, M. Baryakhtar, J. Huang, A. Roshko, G. Burton, M. Colangelo, K. V. Tilburg, A. Arvanitaki, S. W. Nam and K. K. Berggren, “First Constraints on Dark Photon Dark Matter with Superconducting Nanowire Detectors in an Optical Haloscope,” *arXiv:2110.01582,* 2021.

[189] C. Schuck, W. H. P. Pernice, X. Ma and H. X. Tang, “Optical time domain reflectometry with low noise waveguide-coupled superconducting nanowire single-photon detectors,” *Applied Physics Letters,* vol. 102, p. 191104, 2013.

[190] G. Overton, “Ariane 6 launch program chooses ID Quantique single-photon-counting technology,” 17 December 2017. [Online]. Available: https://www.laserfocusworld.com/test-measurement/test-measurement/article/16569515/ariane-6-launch-program-chooses-id-quantique-singlephotoncounting-technology.

[191] M. G. Tanner, S. D. Dyer, B. Baek, R. H. Hadfield and S. W. Nam, “High-resolution single-mode fiber-optic distributed Raman sensor for absolute temperature measurement using superconducting nanowire single-photon detectors,” *Applied Physics Letters,* vol. 99, p. 201110, 2011.

[192] S. D. Dyer, M. G. Tanner, B. Baek, R. H. Hadfield and S. W. Nam, “Analysis of a distributed fiber-optic temperature sensor using single-photon detectors,” *Opt. Express,* vol. 20, p. 3456–3466, February 2012.

[193] A. McCarthy, N. J. Krichel, N. R. Gemmell, X. Ren, M. G. Tanner, S. N. Dorenbos, V. Zwiller, R. H. Hadfield and G. S. Buller, “Kilometer-range, high resolution depth imaging via 1560 nm wavelength single-photon detection,” *Opt. Express,* vol. 21, p. 8904–8915, April 2013.

[194] G. G. Taylor, A. McCarthy, B. Korzh, A. D. Beyer, D. Morozov, R. M. Briggs, J. P. Allmaras, B. Bumble, M. D. Shaw, R. H. Hadfield and G. S. Buller, “Long-range depth imaging with 13ps temporal resolution using a superconducting nanowire singlephoton detector,” in *Conference on Lasers and Electro-Optics*, 2020.

[195] G. G. Taylor, D. Morozov, N. R. Gemmell, K. Erotokritou, S. Miki, H. Terai and R. H. Hadfield, “Photon counting LIDAR at 2.3µm wavelength with superconducting nanowires,” *Opt. Express,* vol. 27, p. 38147–38158, December 2019.

[196] P. Szypryt, S. R. Meeker, G. Coiffard, N. Fruitwala, B. Bumble, G. Ulbricht, A. B. Walter, M. Daal, C. Bockstiegel, G. Collura, N. Zobrist, I. Lipartito and B. A. Mazin, “Large-format platinum silicide microwave kinetic inductance detectors for optical to near-IR astronomy,” *Opt. Express,* vol. 25, p. 25894–25909, October 2017.

[197] A. V. Sergeev, V. V. Mitin and B. S. Karasik, “Ultrasensitive hot-electron kinetic-inductance detectors operating well below the superconducting transition,” *Appl. Phys. Lett.,* vol. 80, pp. 817-819, 2002.

[198] H. G. Leduc, B. Bumble, P. K. Day, B. H. Eom, J. Gao, S. Golwala, B. A. Mazin, S. McHugh, A. Merrill, D. C. Moore, O. Noroozian, A. D. Turner and J. Zmuidzinas, “Titanium nitride films for ultrasensitive microresonator detectors,” *Appl. Phys. Lett.,* vol. 97, p. 102509, 2010.

[199] P. J. de Visser, J. J. A. Baselmans, P. Diener, S. J. C. Yates, A. Endo and T. M. Klapwijk, “Number Fluctuations of Sparse Quasiparticles in a Superconductor,” *Phys. Rev. Lett.,* vol. 106, no. 16, p. 167004, April 2011.

[200] Monfardini, A. and Swenson, L. J. and Bideaud, A. and Désert, F. X. and Yates, S. J. C. and Benoit, A. and Baryshev, A. M. and Baselmans, J. J. A. and Doyle, S. and Klein, B. and Roesch, M. and Tucker, C. and Ade, P. and Calvo, M. and Camus, P. and Giordano, C. and Guesten, R. and Hoffmann, C. and Leclercq, S. and Mauskopf, P. and Schuster, K. F., "NIKA: A millimeter-wave kinetic inductance camera," *Astronomy & Astrophysics*, vol. 521, p. A29, 2010.

[201] N. Zobrist, G. Coiffard, B. Bumble, N. Swimmer, S. Steiger, M. Daal, G. Collura, A. B. Walter, C. Bockstiegel, N. Fruitwala, I. Lipartito and B. A. Mazin, "Design and performance of hafnium optical and near-IR kinetic inductance detectors," *Applied Physics Letters*, vol. 115, p. 213503, 2019.

[202] P. J. de Visser, S. A. H. de Rooij, V. Murugesan, D. J. Thoen and J. J. A. Baselmans, "Phonon-Trapping-Enhanced Energy Resolution in Superconducting Single-Photon Detectors," *Phys. Rev. Applied*, vol. 16, no. 3, p. 034051, September 2021.

[203] J. D. A. Parrianen, A. Papageorgiou, S. Doyle and E. Pascale, "Modelling the Performance of Single-Photon Counting Kinetic Inductance Detectors," *Journal of Low Temperature Physics*, vol. 193, p. 113–119, 2018.

[204] F. Arams, C. Allen, B. Peyton and E. Sard, "Millimeter Mixing and Detection in Bulk InSb," *Proceedings of the IEEE*, vol. 54, pp. 612-624, April 1966.

[205] T. G. Phillips and K. B. Jefferts, "A Low Temperature Bolometer Heterodyne Receiver for Millimeter Wave Astronomy," *Review of Scientific Instruments*, vol. 44, pp. 1009-1014, August 1973.

[206] E. M. Gershenzon, “Millimeter and submillimeter range mier based on electronic heating of superconducting films in the resistive state,” *Sov. Phys. Supercond.,* vol. 3, pp. 1582-1597, 1990.

[207] K. S. Il’in, I. I. Milostnaya, A. A. Verevkin, G. N. Gol’tsman, E. M. Gershenzon and R. Sobolewski, “Ultimate quantum efficiency of a superconducting hot-electron photodetector,” *Applied Physics Letters,* vol. 73, pp. 3938-3940, 1998.

[208] D. E. Prober, “Superconducting terahertz mixer using transition-edge microbolometer,” *Appl. Phys. Lett.,* vol. 62, p. 2119, April 1993.

[209] B. S. Karasik, W. R. McGrath and R. A. Wyss, “Optimal choice of material for HEB superconducting mixers,” *Applied Superconductivity, IEEE Transactions on,* vol. 9, pp. 4213-4216, June 1999.

[210] D. Golubev and L. Kuzmin, “Nonequilibrium theory of a hot-electron bolometer with normal metal-insulator-superconductor tunnel junction,” *Journal of Applied Physics,* vol. 89, pp. 6464-6472, 2001.

[211] B. S. Karasik, S. V. Pereverzev, A. Soibel, D. F. Santavicca, D. E. Prober, D. Olaya and M. E. Gershenson, “Energy-resolved detection of single infrared photons with λ = 8μm using a superconducting microbolometer,” *Applied Physics Letters*, vol. 101, p. 052601, 2012.

[212] F. Martini, S. Cibella, A. Gaggero, F. Mattioli and R. Leoni, “Waveguide integrated hot electron bolometer for classical and quantum photonics,” *Opt. Express,* vol. 29, p. 7956–7965, March 2021.